PHYSICAL REVIEW D **92,** 074503 (2015)

Calculation of $K \to \pi\pi$ decay amplitudes with improved Wilson fermion action in lattice QCD

N. Ishizuka,[1,2] K.-I. Ishikawa,[3] A. Ukawa,[4] and T. Yoshié[1,2]

[1]*Center for Computational Sciences, University of Tsukuba, Tsukuba, Ibaraki 305-8577, Japan*
[2]*Graduate School of Pure and Applied Sciences, University of Tsukuba, Tsukuba, Ibaraki 305-8571, Japan*
[3]*Department of Physics, Hiroshima University, Higashi-Hiroshima, Hiroshima 739-8526, Japan*
[4]*RIKEN Advanced Institute for Computational Science, Kobe 650-0047, Japan*

(Received 1 June 2015; published 7 October 2015)

We present our result for the $K \to \pi\pi$ decay amplitudes for both the $\Delta I = 1/2$ and $3/2$ processes with the improved Wilson fermion action. Expanding on the earlier works by Bernard *et al.* and by Donini *et al.*, we show that mixings with four-fermion operators with wrong chirality are absent even for the Wilson fermion action for the parity odd process in both channels due to CPS symmetry. Therefore, after subtraction of an effect from the lower dimensional operator, a calculation of the decay amplitudes is possible without complications from operators with wrong chirality, as for the case with chirally symmetric lattice actions. As a first step to verify the possibility of calculations with the Wilson fermion action, we consider the decay amplitudes at an unphysical quark mass $m_K \sim 2m_\pi$. Our calculations are carried out with $N_f = 2 + 1$ gauge configurations generated with the Iwasaki gauge action and nonperturbatively $O(a)$-improved Wilson fermion action at $a = 0.091$ fm, $m_\pi = 280$ MeV, and $m_K = 580$ MeV on a $32^3 \times 64$ ($La = 2.9$ fm) lattice. For the quark loops in the penguin and disconnected contributions in the $I = 0$ channel, the combined hopping parameter expansion and truncated solver method work very well for variance reduction. We obtain, for the first time with a Wilson-type fermion action, that $\mathrm{Re}A_0 = 60(36) \times 10^{-8}$ GeV and $\mathrm{Im}A_0 = -67(56) \times 10^{-12}$ GeV for a matching scale $q^* = 1/a$. The dependence on the matching scale q^* for these values is weak.

DOI: 10.1103/PhysRevD.92.074503 PACS numbers: 11.15.Ha, 12.38.Gc, 13.25.Es

I. INTRODUCTION

Calculation of the $K \to \pi\pi$ decay amplitudes is very important to quantitatively understand the $\Delta I = 1/2$ rule in the decay of the neutral K meson system and to theoretically predict the direct CP violation parameter (ϵ'/ϵ) from the Standard Model. A direct lattice QCD calculation of the decay amplitudes for the $\Delta I = 3/2$ process has been attempted for a long time. Recently, the RBC-UKQCD Collaboration presented the results at the physical quark mass in Ref. [1], and those in the continuum limit in Ref. [2] in the physical kinematics, where the pions in the final state have finite momenta. They used the domain wall fermion action which preserves chiral symmetry on the lattice.

A direct calculation of the decay amplitudes for the $\Delta I = 1/2$ process has been unsuccessful for a long time, due to large statistical fluctuations from the disconnected diagrams. A first direct calculation was reported by the RBC-UKQCD Collaboration in Ref. [3] at a lattice spacing $a = 0.114$ fm and a pion mass $m_\pi = 422$ MeV on a $16^3 \times 32$ lattice with the domain wall fermion action. They also presented a result at a smaller quark mass ($m_\pi = 330$ MeV) on a $24^3 \times 64$ lattice with the same fermion action at Lattice 2011 [4]. In these two calculations, the kinematics was a K meson at rest decaying to two zero momentum pions at an unphysical quark mass satisfying $m_K \sim 2m_\pi$. The RBC-UKQCD Collaboration has since been attempting a direct calculation in the physical kinematics at the physical quark mass by utilizing G-parity boundary conditions. Their preliminary result was reported at Lattice 2014 [5].

An aim of the present article is to report on our calculation of the $K \to \pi\pi$ decay amplitudes with the improved Wilson fermion action for both the $\Delta I = 1/2$ and $3/2$ processes. That such a calculation is feasible stems from a realization, as shown in the present article, that CPS symmetry [6] and its extensions [7] ensure that mixings with four-fermion operators with wrong chirality are absent even for the Wilson fermion action for the parity odd process in both channels. A mixing to a lower dimension operator does occur, which gives unphysical contributions to the amplitudes on the lattice. However, it can be nonperturbatively subtracted by imposing a renormalization condition [8,9]. After the subtraction, we can obtain the physical decay amplitudes by the renormalization factor having the same structure as for the chiral symmetry preserved case. A potential advantage with the Wilson fermion action over chirally symmetric lattice actions such as the domain wall action is that the computational cost is generally smaller. Hence, with the same amount of computational resources, a statistical improvement may be expected with the lattice calculation of the decay amplitudes, albeit this point has to be verified by actual calculations.

In the present work, we consider the decay of K meson to two zero momentum pions at an unphysical quark mass $m_K \sim 2m_\pi$, as in Refs. [3,4], as the first step of a study with the Wilson fermion action. Our calculations are carried out on a subset of gauge configurations previously generated by the PACS-CS Collaboration with the Iwasaki gauge action and the nonperturbatively $O(a)$-improved Wilson fermion action for $N_f = 2+1$ flavors at $\beta = 1.9$ on a $32^3 \times 64$ lattice [10]. The subset corresponds to the hopping parameters $\kappa_{ud} = 0.13770$ for the up and the down quark, and $\kappa_s = 0.13640$ for the strange quark. We further generate gauge configurations at the same parameters to improve the statistics. The total number of gauge configurations used in the present work is 480. The parameters determined from the hadron spectrum analysis are $a = 0.091$ fm for the lattice spacing, $La = 2.91$ fm for the lattice size, $m_\pi = 275.7(1.5)$ MeV, and $m_K = 579.7(1.3)$ MeV for the pion and the K masses. The energy of the two-pion state is shifted from $2m_\pi$ by the two-pion interaction on the lattice. The energy difference between the initial K meson and the final two-pion state takes a nonzero value, $\Delta E = 21(3)$ MeV for the $I = 2$ channel, and $36(18)$ MeV for the $I = 0$ channel on these configurations. In the present work, we assume that these mismatches of the energy give only small effects to the decay amplitudes.

This paper is organized as follows. The $K \to \pi\pi$ decay amplitudes can be calculated from the product of the $K \to \pi\pi$ matrix elements of the $\Delta S = 1$ four-fermion weak interaction operators and the Wilson coefficient functions for the operator product expansion. In Sec. II, these four-fermion operators are introduced and the operator mixing among them for the Wilson fermion action is discussed. In Sec. III, we describe the method of calculation used in the present work. The simulation parameters are also given. We present our results in Sec. IV and compare them with those by the RBC-UKQCD Collaboration and the experimental values. Conclusions of the present work are given in Sec. V.

Our calculations have been carried out on the PACS-CS computer and T2K-Tsukuba at University of Tsukuba, the K computer at the RIKEN Advanced Institute for Computational Science, SR16000 at University of Tokyo, and SR16000 at High energy Accelerator Research Organization (KEK). Our preliminary results have been reported at Lattice 2013 and 2014 [11].

II. $\Delta S = 1$ OPERATORS

A. $\Delta S = 1$ weak operators in the continuum theory

The effective Hamiltonian of the $K \to \pi\pi$ decay in the continuum theory can be written as [12]

$$H = \frac{G_F}{\sqrt{2}}(V_{us}^* V_{ud}) \sum_{i=1}^{10} (z_i(\mu) + \tau y_i(\mu)) Q_i(\mu), \quad (1)$$

with $\tau = -(V_{ts}^* V_{td})/(V_{us}^* V_{ud})$, and $z_i(\mu)$ and $y_i(\mu)$ $(i = 1, 2, \ldots, 10)$ are the coefficient functions at renormalization scale μ. Here, we consider the case $\mu \le m_c$, where three light quarks, up, down, and strange, are the active quarks in the theory. The ten operators $Q_i(\mu)$ $(i = 1, 2, \ldots, 10)$ denote the $\Delta S = 1$ four-fermion operators renormalized at μ, which are given by

$$Q_1 = (\bar{s}d)(\bar{u}u)_{LL}, \quad (2)$$

$$Q_2 = (\bar{s} \times d)(\bar{u} \times u)_{LL}, \quad (3)$$

$$Q_3 = (\bar{s}d)\sum_q (\bar{q}q)_{LL}, \quad (4)$$

$$Q_4 = (\bar{s} \times d)\sum_q (\bar{q} \times q)_{LL}, \quad (5)$$

$$Q_5 = (\bar{s}d)\sum_q (\bar{q}q)_{LR}, \quad (6)$$

$$Q_6 = (\bar{s} \times d)\sum_q (\bar{q} \times q)_{LR}, \quad (7)$$

$$Q_7 = \frac{3}{2}(\bar{s}d)\sum_q e_q (\bar{q}q)_{LR}, \quad (8)$$

$$Q_8 = \frac{3}{2}(\bar{s} \times d)\sum_q e_q (\bar{q} \times q)_{LR}, \quad (9)$$

$$Q_9 = \frac{3}{2}(\bar{s}d)\sum_q e_q (\bar{q}q)_{LL}, \quad (10)$$

$$Q_{10} = \frac{3}{2}(\bar{s} \times d)\sum_q e_q (\bar{q} \times q)_{LL}, \quad (11)$$

where $(\bar{s}d)(\bar{u}u)_{L,R/L} = (\bar{s}\gamma_\mu(1-\gamma_5)d)(\bar{u}\gamma_\mu(1 \pm \gamma_5)u)$, and $\times$ means the contraction of color indices according to $(\bar{s} \times d)_L(\bar{u} \times d)_L = \sum_{a,b}(\bar{s}_a d_b)_L(\bar{u}_b d_a)_L$. The summation for q is taken for the active quarks $(q = u, d, s)$ and the electric charge takes values $e_u = +2/3$ and $e_d = e_s = -1/3$.

In the four-dimensional space-time, these operators are not all independent, satisfying the relations

$$Q_4 = -Q_1 + Q_2 + Q_3, \quad (12)$$

$$Q_9 = (3Q_1 - Q_3)/2, \quad (13)$$

$$Q_{10} = (3Q_2 - Q_4)/2 = Q_2 + (Q_1 - Q_3)/2, \quad (14)$$

due to the Fierz identity. In general dimensions, however, these relations are not valid. Therefore, if we adopt the dimensional regularization for regularization, we should deal with all operators Q_i for $i = 1, 2, \ldots, 10$ as independent.

B. Operator mixing for the Wilson fermion action

The matrix elements calculated on the lattice are converted to those in the continuum by the renormalization factor for the operators. In this section, we discuss the renormalization factor in the case of the Wilson fermion action.

As already mentioned in Sec. II A, the ten four-fermion operators Q_i are not independent, and they may be arranged into seven linearly independent combinations according to the irreducible representation of the flavor $\mathrm{SU}(3)_L \times \mathrm{SU}(3)_R$ symmetry group. The seven operators consist of $(\mathbf{27},\mathbf{1}) + 4\cdot(\mathbf{8},\mathbf{1}) + 2\cdot(\mathbf{8},\mathbf{8})$, whose components are given by

$$(\mathbf{27},\mathbf{1}) \quad Q'_1 = 3Q_1 + 2Q_2 - Q_3, \tag{15}$$

$$\begin{aligned}(\mathbf{8},\mathbf{1}) \quad & Q'_2 = 2Q_1 - 2Q_2 + Q_3,\\ & Q'_3 = -3Q_1 + 3Q_2 + Q_3,\\ & Q_5, \qquad Q_6,\end{aligned} \tag{16}$$

$$(\mathbf{8},\mathbf{8}) \quad Q_7, \qquad Q_8. \tag{17}$$

The operators $Q'_{1,2,3}$ are the LL type four-fermion operators and $Q_{5,6,7,8}$ are of LR type.

If the chiral symmetry is preserved in the regularization, mixings between operators in different representations are forbidden. For the Wilson fermion action, however, chiral symmetry is broken to the vector subgroup, $\mathrm{SU}(3)_L \times \mathrm{SU}(3)_R \to \mathrm{SU}(3)_V$. Hence, mixings among different representations is in general allowed, and new operators arise through radiative corrections. However, we show below that such a problem is absent for the parity odd part of the operators in the list of (2)–(11) or of (15)–(17) for the Wilson fermion action employed in the present work.

To investigate the operator mixing, we exploit the full set of unbroken symmetries for the Wilson fermion action, namely, flavor $\mathrm{SU}(3)_V$, parity P, charge conjugation C, and CPS which is the symmetry under CP transformation followed by the exchange of the d and the s quarks. All operators in the list (15)–(17) are $CPS = +1$ operators, but the following operators also have the same quantum numbers including CPS,

$$Q_X = (\bar{s}d)(\bar{d}d - \bar{s}s)_{SP+PS}, \tag{18}$$

$$Q_Y = (\bar{s}\times d)(\bar{d}\times d - \bar{s}\times s)_{SP+PS}, \tag{19}$$

where $(\bar{s}d)(\bar{d}d)_{SP+PS} = (\bar{s}d)_S(\bar{d}d)_P + (\bar{s}d)_P(\bar{d}d)_S$ and $(\bar{s}d)_S = \bar{s}d$ and $(\bar{s}d)_P = \bar{s}\gamma_5 d$. Therefore, we have to consider mixings including these operators.

Let us discuss the problem in two steps, first considering mixings through diagrams in which gluons are exchanged between quarks of the four-fermion operators (gluon exchange diagrams), and second through penguin diagrams in which a pair of quarks from the four-fermion operators forms a quark loop.

For the first type of mixings, it was shown in Ref. [7] that the parity odd part of the LL and LR type operators, and the $SP + PS$ type operator do not mix with each other. One can prove this through the use of CPS, CPS', and CPS'' symmetries which holds for the gluon exchange diagrams, where S' and S'' are the flavor switching for a four-fermion operator $(\bar{\psi}_1\psi_2)(\bar{\psi}_3\psi_4)_{\Gamma_1\Gamma_2}$ or $(\bar{\psi}_1\times\psi_2)(\bar{\psi}_3\times\psi_4)_{\Gamma_1\Gamma_2}$ defined by

$$S'\colon \psi_1 \leftrightarrow \psi_2, \qquad \psi_3 \leftrightarrow \psi_4, \tag{20}$$

$$S''\colon \psi_1 \leftrightarrow \psi_4, \qquad \psi_2 \leftrightarrow \psi_3. \tag{21}$$

The parity odd part of the LL and LR type operators in (15)–(17), which are of $-VA - AV$ and $VA - AV$ type, and that of $Q_{X,Y}$ in (18)–(19), which is of $SP + PS$ type, are eigenvectors of the CPS' and CPS'' symmetry with a different set of eigenvalues,

$$\begin{array}{rccc} & & CPS' & CPS'' \\ LL|_{P=-1} = & -VA - AV & +1 & +1, \\ LR|_{P=-1} = & VA - AV & +1 & -1, \\ & SP + PS & -1 & -1. \end{array} \tag{22}$$

Therefore, $Q_{X,Y}$ (the $SP + PS$ type) do not mix with the operators (15)–(17) (the LL and the LR type).

Furthermore, the operators $Q_{7,8} \in (\mathbf{8},\mathbf{8})$ (the LR type) do not mix with the LL type operators $[Q'_{1,2,3} \in (\mathbf{27},\mathbf{1}), (\mathbf{8},\mathbf{1})]$, or with $Q_{5,6} \in (\mathbf{8},\mathbf{1})$ (the LR type) because the gluon exchange diagrams do not change the flavor structure.

In addition, the mixing between the (27,1) and (8,1) representations is forbidden by the flavor $\mathrm{SU}(3)_V$ symmetry. To sum up, the matrix of the renormalization factor for the gluon exchange diagrams has the same structure as in the chiral symmetry preserved case.

Next, we investigate the possibility of unwanted mixings though the penguin diagrams. In the penguin diagrams for $Q_{7,8} \in (\mathbf{8},\mathbf{8})$, a cancellation of the quark loop at the weak operator occurs between the d quark and the s quark contributions. This can be seen as the following. The penguin diagram for the parity odd part of the operators Q_7, except for the contribution from the spectator quarks, can be written as

$$C_7 = C_{VA} - C_{AV}, \tag{23}$$

where

$$C_{\Gamma_1\Gamma_2} = \mathrm{T}[s(X)(\bar{s}d)(\bar{u}u - \bar{d}d/2 - \bar{s}s/2)_{\Gamma_1\Gamma_2}(x)\bar{d}(Y)], \tag{24}$$

at the space-time position x, with the external s quark $s(X)$ at X, and the d quark $d(Y)$ at Y. Rewriting with the quark propagator $Q_q(x,y)$ for the quark q, we obtain,

$$\begin{aligned} C_{\Gamma_1\Gamma_2} &= +Q_s(X,x)\Gamma_1 Q_d(x,Y)\mathrm{Tr}[(-Q_u(x,x)+Q_d(x,x)/2+Q_s(x,x)/2)\Gamma_2] \\ &\quad - Q_s(X,x)\Gamma_1 Q_d(x,x)\Gamma_2 Q_d(x,Y)/2 - Q_s(X,x)\Gamma_2 Q_s(x,x)\Gamma_1 Q_d(x,Y)/2. \end{aligned} \tag{25}$$

Using the isospin symmetry $Q_u = Q_d$, C_7 can be written by

$$\begin{aligned} C_7 &= C_{VA} - C_{AV} \\ &= [-Q_s(X,x)\gamma_\mu Q_d(x,Y)\mathrm{Tr}[(Q_d(x,x)-Q_s(x,x))\gamma_\mu\gamma_5]/2 \\ &\quad - Q_s(X,x)\gamma_\mu Q_d(x,x)\gamma_\mu\gamma_5 Q_d(x,Y)/2 - Q_s(X,x)\gamma_\mu\gamma_5 Q_s(x,x)\gamma_\mu Q_d(x,Y)/2] \\ &\quad - [-Q_s(X,x)\gamma_\mu\gamma_5 Q_d(x,Y)\mathrm{Tr}[(Q_d(x,x)-Q_s(x,x))\gamma_\mu]/2 \\ &\quad - Q_s(X,x)\gamma_\mu\gamma_5 Q_d(x,x)\gamma_\mu Q_d(x,Y)/2 - Q_s(X,x)\gamma_\mu Q_s(x,x)\gamma_\mu\gamma_5 Q_d(x,Y)/2] \\ &= -Q_s(X,x)\gamma_\mu Q_d(x,Y)\mathrm{Tr}[Q_{ds}(x,x)\gamma_\mu\gamma_5]/2 + Q_s(X,x)\gamma_\mu\gamma_5 Q_d(x,Y)\mathrm{Tr}[(Q_{ds}(x,x)\gamma_\mu]/2 \\ &\quad - Q_s(X,x)\gamma_\mu Q_{ds}(x,x)\gamma_\mu\gamma_5 Q_d(x,Y)/2 + Q_s(X,x)\gamma_\mu\gamma_5 Q_{ds}(x,x)\gamma_\mu Q_d(x,Y)/2, \end{aligned} \tag{26}$$

where $Q_{ds}(x,x) = Q_d(x,x) - Q_s(x,x)$. Here, we see that a cancellation of the quark loops at the weak operator occurs between the d quark and the s quark contributions. We can see this cancellation also in the operator Q_8.

Since this cancellation means that the renormalization factor coming from the penguin diagram is proportional to the quark mass difference $(m_d - m_s)$, mixings to four-fermion operators are absent due to the dimensional reason. In addition, the operator arising from the penguin diagrams should have the flavor structure $(\bar{s}d)(\bar{u}u + \bar{d}d + \bar{s}s)$, which is different from that of $Q_{7,8}$. Thus, operator mixings from $Q_{7,8} \in (\mathbf{8},\mathbf{8})$ to the other representations and their reverse are absent. These statements also hold for $Q_{X,Y}$ in (18)–(19) for the same reason, and the operators $Q_{X,Y}$ are fully isolated in the theory. Further mixing between the $(\mathbf{27},\mathbf{1})$ and $(\mathbf{8},\mathbf{1})$ representations in the penguin diagrams is forbidden by the flavor $\mathrm{SU}(3)_V$ symmetry. This concludes the proof on the absence of unwanted mixings among the parity-odd part of dimension 6 operators.

Up to now, we have shown that the matrix of the renormalization factor for the parity odd part of the four-fermion operators in (15)–(17) have the same structure as that in the chiral symmetry preserved case. Here, we consider the mixing to lower dimensional operators. From *CPS* symmetry and the equation of motion of the quark, there is only one operator with the dimension less than 6, which is

$$Q_P = (m_d - m_s)\cdot\bar{s}\gamma_5 d. \tag{27}$$

This operator also appears in the continuum, but does not yield a nonvanishing contribution to the physical decay amplitudes, since it is a total derivative operator. However, this is not valid for the Wilson fermion action due to chiral symmetry breaking by the Wilson term, and the operator (27) does give a nonzero unphysical contribution to the amplitudes on the lattice. This contribution should be subtracted nonperturbatively because the mixing coefficient includes a power divergence due to the lattice cutoff growing as $1/a^2$. In the present work, we subtract it by imposing the following condition [8,9],

$$\langle 0|\bar{Q}_i|K\rangle = \langle 0|Q_i - \beta_i\cdot Q_P|K\rangle = 0, \tag{28}$$

for each operator Q_i in (2)–(6). The matrix of the renormalization factor of the subtracted operators $\bar{Q}_i$ has the same structure as in the chiral symmetry preserved case.

Here, we mention an ambiguity in the subtraction procedure. Instead of strictly demanding the subtraction condition (28), we can choose a different subtracted operator, $\bar{Q}'_i = \bar{Q}_i + \beta'_i\cdot Q_P$, where β'_i is a finite constant depending on the quark masses. The constants do not include the power divergence, and they vanish in the chiral limit. In general, such a finite ambiguity seems to remain in the final results of the decay amplitude for finite quark masses, as pointed out in Ref. [9]. Our case, however, is not a such case for the following reason. The operator Q_P can be written as $Q_P = (m_d - m_s)/(m_d + m_s)\cdot(\partial_\mu A_\mu - a\bar{X}_A)$ from the relation of the partially conserved axial vector current for the Wilson fermion action, where A_μ is the renormalized axial vector current and $\bar{X}_A$ is the dimension 5 operator whose matrix element vanishes in the continuum limit. Thus, a $\beta'_i\cdot Q_P$ term yields a contribution of form $\Delta p\cdot C - \langle\pi\pi|a\bar{X}_A|K\rangle\cdot D$ to the decay amplitude with finite constants C and D, where Δp is the momentum difference between the initial and the final state. These contributions do not include any power divergent parts. Thus, by taking $\Delta p \to 0$ and the continuum limit, we can safely estimate the physical value of the decay amplitudes without suffering from the ambiguity.

III. METHOD

A. Simulation parameters

Our calculations are carried out on a subset of gauge configurations previously generated by PACS-CS Collaboration with the Iwasaki gauge action and non-perturbatively $O(a)$-improved Wilson fermion action at $\beta = 1.9$ on a $32^3 \times 64$ lattice [10]. The subset corresponds to the hopping parameters $\kappa_{ud} = 0.13770$ for the up and the down quark, and $\kappa_s = 0.13640$ for the strange quark. In order to improve the statistics, we further generate gauge configurations by two runs of the simulation. The first run uses the same algorithm as employed at the same parameters in Ref. [10]. The trajectory length is $\tau = 1/4$ and the dead or alive link method with random parallel translation is used. The length of MD time, *i.e.*, the number of trajectories multiplied by the trajectory length τ, of this run is 6000 units as compared to 2000 for the original run of Ref. [10]. The second run does not use the dead (alive) link method. All links are active, the trajectory length equals $\tau = 1$, and the length of run is also 6000 MD time units. We measure hadron Green's functions and the decay amplitudes at every 25 MD time units for both runs. The total length of the run is 12,000 MD time units, and the total number of gauge configurations employed for the measurement is 480.

We estimate statistical errors by the jackknife method with bins of ten configurations (250 MD time units). The parameters determined from the spectrum analysis are $a = 0.091$ fm for lattice spacing, $La = 2.91$ fm for spatial lattice size, and $m_\pi = 275.7(1.5)$ MeV and $m_K = 579.7(1.3)$ MeV for the pion and the K meson masses.

In the present work, we consider the decay in the unphysical kinematics, where the K meson decay to two zero momentum pions. The energy difference between the initial K meson and the final two-pion state is $\Delta E \equiv m_K - E^I_{\pi\pi} = 21(3)$ MeV for $I = 2$ and 36(18) MeV for $I = 0$ on our configurations as shown in the following section. In the present work, we assume that these mismatches of the energy give only small effects to the decay amplitudes.

B. Time correlation function for $K \to \pi\pi$

We extract the matrix element $\langle K|\bar{Q}_i|\pi\pi; I\rangle$ from the time correlation function for the $K \to \pi\pi$ process,

$$G^I_i(t) = \frac{1}{T}\sum_{\delta=0}^{T-1}\langle 0|W_{K^0}(t_K+\delta)\bar{Q}_i(t+\delta) \times W^I_{\pi\pi}(t_\pi+\delta, t_\pi+1+\delta)|0\rangle. \quad (29)$$

Let us describe various features of this definition one by one. Firstly, $\bar{Q}_i(t)$ is the subtracted weak operator at the time slice t defined by

$$\bar{Q}_i(t) = \sum_{\mathbf{x}} \bar{Q}_i(\mathbf{x}, t), \quad (30)$$

with the subtracted operator $\bar{Q}_i(\mathbf{x}, t)$ at the space-time position $(\mathbf{x}, t)$ defined in (28).

Secondly, the operator $W_{K^0}(t)$ is the wall source for the K^0 meson at the time slice t,

$$W_{K^0}(t) = -\bar{W}_d(t)\gamma_5 W_s(t), \quad (31)$$

with the wall source for the quark $q = u, d, s$,

$$W_q(t) = \sum_{\mathbf{x}} q(\mathbf{x}, t), \quad (32)$$

$$\bar{W}_q(t) = \sum_{\mathbf{x}} \bar{q}(\mathbf{x}, t). \quad (33)$$

We adopt $K^0 = -\bar{d}\gamma_5 s$ as the neutral K meson operator, so our correlation function has an extra minus from the usual convention.

Thirdly, the operator $W^I_{\pi\pi}(t_1, t_2)$ in (29) is the wall source for the two-pion state with the isospin I, which is defined by

$$W^{I=2}_{\pi\pi}(t_1, t_2) = [(W_{\pi^0}(t_1)W_{\pi^0}(t_2) + W_{\pi^+}(t_1)W_{\pi^-}(t_2))/\sqrt{3} + (t_1 \leftrightarrow t_2)]/2, \quad (34)$$

$$W^{I=0}_{\pi\pi}(t_1, t_2) = [(-W_{\pi^0}(t_1)W_{\pi^0}(t_2)/\sqrt{2} + \sqrt{2}W_{\pi^+}(t_1)W_{\pi^-}(t_2))/\sqrt{3} + (t_1 \leftrightarrow t_2)]/2, \quad (35)$$

where $W_{\pi^i}(t)$ is the wall source for π^i meson at the time slice t,

$$W_{\pi^+}(t) = -\bar{W}_d(t)\gamma_5 W_u(t), \quad (36)$$

$$W_{\pi^0}(t) = (\bar{W}_u(t)\gamma_5 W_u(t) - \bar{W}_d(t)W_d(t))/\sqrt{2}, \quad (37)$$

$$W_{\pi^-}(t) = \bar{W}_u(t)\gamma_5 W_d(t). \quad (38)$$

The wall source of each pion is separated by one lattice unit according to $t_1 = t_\pi$ and $t_2 = t_\pi + 1$ in (29) to avoid contamination from Fierz-rearranged terms.

We impose the periodic boundary condition in all directions. The summation over δ, where $T = 64$ denotes the temporal size of the lattice, is taken in (29) to improve the statistics. The time slice of the K meson is set at $t_K = 24$ and that of the two pion at $t_\pi = 0$. The gauge configurations are fixed to the Coulomb gauge at the time slice of the wall source $t_K + \delta$, $t_1 + \delta$ and $t_2 + \delta$ for each δ.

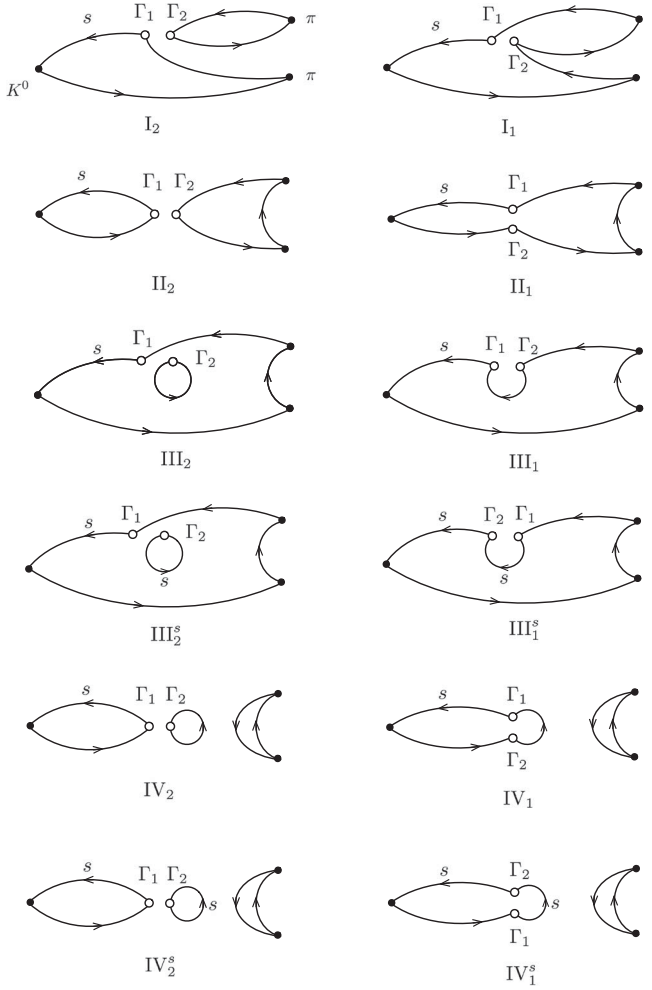

FIG. 1. Quark contractions for the time correlation function for the $K \to \pi\pi$ process for the operator Q_i $(i = 1, 2, \ldots, 10)$.

In the calculation of the mixing coefficient of the lower dimensional operator, we rewrite the subtraction of the lower dimensional operator (28) as

$$\bar{Q}_i = Q_i - \beta_i \cdot Q_P = Q_i - \alpha_i \cdot P, \tag{39}$$

by (27), with $P = \bar{s}\gamma_5 d$ and $\alpha_i = (m_d - m_s) \cdot \beta_i$. The mixing coefficient α_i in (39) is obtained from the following ratio of the time correlation function,

$$\alpha_i = \sum_{\delta_1=0}^{T-1} \langle 0|W_{K^0}(t_K + \delta_1) Q_i(t + \delta_1)|0\rangle \Big/ \sum_{\delta_2=0}^{T-1} \langle 0|W_{K^0}(t_K + \delta_2) P(t + \delta_2)|0\rangle, \tag{40}$$

in the large $t_K - t$ region, where $P(t) = \sum_{\mathbf{x}} P(\mathbf{x}, t)$.

C. Quark contractions for $K \to \pi\pi$ and $K \to 0$

In Fig. 1, we list all of the possible quark contractions for the $K \to \pi\pi$ time correlation function $G_i^I(t)$ in (29). Again there are a number of features, so let us describe them one by one.

(1) Time runs from right to left in the diagrams.
(2) There are four types of contractions labeled I, II, III, and IV.
(3) The diagrams show the quark contractions for the four-fermion operator

$$Q = \sum_{a,b,c,d} (\bar{\psi}_a^1 \Gamma_1 \psi_b^2)(\bar{\psi}_c^3 \Gamma_2 \psi_d^4) T_{abcd} \tag{41}$$

with the color indices a, b, c, d, where the spin matrix $\Gamma_{1,2}$ and the color matrix T_{abcd} are given, depending on the operator Q_i, as

$$\Gamma_1 = \gamma_\mu(1 - \gamma_5), \quad \Gamma_2 = \gamma_\mu(1 - \gamma_5) \quad \text{for } Q_{1,2,3,4,9,10}, \tag{42}$$

$$\Gamma_1 = \gamma_\mu(1 - \gamma_5), \quad \Gamma_2 = \gamma_\mu(1 + \gamma_5) \quad \text{for } Q_{5,6,7,8}, \tag{43}$$

$$T_{abcd} = \delta_{ab}\delta_{cd} \quad \text{for } Q_{1,3,5,7,9}, \tag{44}$$

$$T_{abcd} = \delta_{ad}\delta_{cb} \quad \text{for } Q_{2,4,6,8,10}. \tag{45}$$

(4) In the diagrams, unmarked line segments represent quark propagators for the u or the d quark, while those marked by "s" are for the strange quark. The filed circles stand for the wall sources for the K meson or pions. The open circles refer to the matrices Γ_1 or Γ_2. The trace for the spin is taken along closed quark lines.
(5) The subscript 1 and 2 attached to the four contraction types I though IV refers to the number of the trace for the spin.
(6) The superscript "s" for the contractions $\mathrm{III}_{1,2}$ and $\mathrm{IV}_{1,2}$ means that the quark loop at the weak operator is for the strange quark.
(7) It should be noted that the location of Γ_1 and Γ_2 for the contraction III_1^s and IV_1^s are switched from those for III_1 and IV_1.
(8) For the contraction IV_i and IV_i^s with $i = 1, 2$ the contribution of the vacuum diagram, $\langle 0|K(t_K)Q_i(t)|0\rangle\langle 0|W_{\pi\pi}^I(t_\pi, t_\pi + 1)|\rangle 0$, should be subtracted.

Let us write down some explicit examples. For the contraction I_2, we have

$$\mathrm{I}_2 = \Bigg[\sum_{a,b,c,d} \sum_{\mathbf{x}} \mathrm{Tr}(W_d(\mathbf{x},t;t_2)\gamma_5 W_d(t_2;\mathbf{x},t)\Gamma_2)_{dc} \times \mathrm{Tr}(W_d(\mathbf{x},t;t_1)\gamma_5 W_d(t_1;t_K)\gamma_5 W_s(t_K;\mathbf{x},t)\Gamma_1)_{ba} \cdot T_{abcd} + (t_1 \leftrightarrow t_2) \Bigg] \Big/ 2, \tag{46}$$

with $t_1 = t_\pi$ and $t_2 = t_\pi + 1$, where the trace is taken for the spin. The three types of W_q $(q = d, s)$ in (46) are the wall source propagators for the quark q defined by

$$W_q(\mathbf{x},t;t_0) = \sum_{\mathbf{y}} Q_q(\mathbf{x},t;\mathbf{y},t_0), \tag{47}$$

$$W_q(t_0;\mathbf{x},t) = \sum_{\mathbf{y}} Q_q(\mathbf{y},t_0;\mathbf{x},t) = \gamma_5 W_q(\mathbf{x},t;t_0)^\dagger \gamma_5, \tag{48}$$

$$W_q(t;t_0) = \sum_{\mathbf{x}} W_q(\mathbf{x},t;t_0), \tag{49}$$

with the quark propagator $Q_q(\mathbf{x},t;\mathbf{y},t_0)$. Similarly, the contraction I_1 is given by

$$\mathrm{I}_1 = \Bigg[\sum_{a,b,c,d} \sum_{\mathbf{x}} \mathrm{Tr}[(W_d(\mathbf{x},t;t_2)\gamma_5 W_d(t_2;\mathbf{x},t)\Gamma_2)_{bc} \times (W_d(\mathbf{x},t;t_1)\gamma_5 W_d(t_1;t_K)\gamma_5 W_s(t_K;\mathbf{x},t)\Gamma_1)_{da}] \cdot T_{abcd} + (t_1 \leftrightarrow t_2) \Bigg] \Big/ 2, \tag{50}$$

where the trace is taken for the spin.

The contraction II_2 is given by

$$\mathrm{II}_2 = \Bigg[\sum_{a,b,c,d} \sum_{\mathbf{x}} \mathrm{Tr}(W_d(\mathbf{x},t;t_2)\gamma_5 W_d(t_2;t_1)\gamma_5 W_d(t_1;\mathbf{x},t)\Gamma_2)_{dc} \times \mathrm{Tr}(W_d(\mathbf{x},t;t_K)\gamma_5 W_s(t_K;\mathbf{x},t)\Gamma_1)_{ba} \cdot T_{abcd} + (t_1 \leftrightarrow t_2) \Bigg] \Big/ 2, \tag{51}$$

and the contraction II_1 is given by

$$\mathrm{II}_1 = \Bigg[\sum_{a,b,c,d} \sum_{\mathbf{x}} \mathrm{Tr}[(W_d(\mathbf{x},t;t_2)\gamma_5 W_d(t_2;t_1)\gamma_5 \times W_d(t_1;\mathbf{x},t)\Gamma_2)_{bc} (W_d(\mathbf{x},t;t_K)\gamma_5 W_s(t_K;\mathbf{x},t)\Gamma_1)_{da}] \cdot T_{abcd} + (t_1 \leftrightarrow t_2) \Bigg] \Big/ 2. \tag{52}$$

The contraction III_2 is given by

$$\mathrm{III}_2 = \Bigg[\sum_{a,b,c,d} \sum_{\mathbf{x}} \mathrm{Tr}(W_d(\mathbf{x},t;t_2)\gamma_5 W_d(t_2;t_1)\gamma_5 \times W_d(t_1;t_K)\gamma_5 W_s(t_K;\mathbf{x},t)\Gamma_1)_{ba} \times \mathrm{Tr}(Q_d(\mathbf{x},t;\mathbf{x},t)\Gamma_2)_{dc} \cdot T_{abcd} + (t_1 \leftrightarrow t_2) \Bigg] \Big/ 2, \tag{53}$$

where the quark loop for the d quark $Q_d(\mathbf{x},t;\mathbf{x},t)$ is calculated by the stochastic method, whose detail is discussed in the next section. The contraction III_2^s is obtained by changing $Q_d(\mathbf{x},t;\mathbf{x},t)$ to the quark loop for the s quark $Q_s(\mathbf{x},t;\mathbf{x},t)$.

Having constructed various quark contractions, we can build the $K \to \pi\pi$ time correlation function $G_i^I(t)$ for the operators Q_i in the isospin channel I in the following way. For the $I = 2$ case, we have

$$G_1^{I=2} = \frac{\sqrt{3}}{3}(\mathrm{I}_2 - \mathrm{I}_1) = G_2^{I=2} = \frac{2}{3} G_9^{I=2} = \frac{2}{3} G_{10}^{I=2}, \tag{54}$$

$$G_7^{I=2} = \frac{\sqrt{3}}{2}(\mathrm{I}_2 - \mathrm{I}_1), \tag{55}$$

$$G_8^{I=2} = \frac{\sqrt{3}}{2}(\mathrm{I}_2 - \mathrm{I}_1), \tag{56}$$

where $\Gamma_{1,2}$ and T_{abcd} in each contractions should be chosen according to (42)–(45) for each operator. The relation among different operators (54) follows from the Fierz identity.

The formulae for the $I = 0$ channel are given as follows:

for $(\bar{s}d)(\bar{u}u) = Q_{1,2}$

$$G^{I=0} = \sqrt{\frac{1}{6}}(-\mathrm{I}_2 - 2\cdot\mathrm{I}_1 + 3\cdot\mathrm{II}_2 + 3\cdot\mathrm{T}_2), \tag{57}$$

for $(\bar{s}d)(\bar{u}u + \bar{d}d + \bar{s}s) = Q_{3,4,5,6}$

$$G^{I=0} = \sqrt{\frac{3}{2}}(-\mathrm{I}_2 + 2\cdot\mathrm{II}_2 - \mathrm{II}_1 + 2\cdot\mathrm{T}_2 - \mathrm{T}_1 + \mathrm{T}_2^s - \mathrm{T}_1^s), \tag{58}$$

for $(\bar{s}d)(\bar{u}u - \bar{d}d/2 - \bar{s}s/2) = Q_{7,8,9,10}$

$$G^{I=0} = \sqrt{\frac{3}{8}}(-\mathrm{I}_2 - \mathrm{I}_1 + \mathrm{II}_2 + \mathrm{II}_1 + \mathrm{T}_2 + \mathrm{T}_1 - \mathrm{T}_2^s + \mathrm{T}_1^s), \tag{59}$$

with $\mathrm{T}_i = \mathrm{III}_i - \mathrm{IV}_i$ and $\mathrm{T}_i^s = \mathrm{III}_i^s - \mathrm{IV}_i^s$ $(i = 1, 2)$, where $\Gamma_{1,2}$ and T_{abcd} in each contractions should be chosen according to (42)–(45) for each operator.

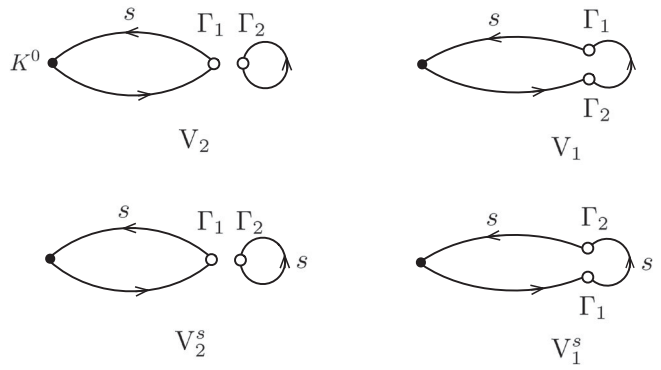

FIG. 2. Quark contractions for the time correlation function for the $K \to 0$ process for the operator Q_i $(i = 1, 2, \ldots, 10)$.

We now turn to the quark contractions needed to subtract the contribution of the lower dimension operator Q_P. In Fig. 2, we list all of the possible quark contractions for the K-to-vacuum time correlation function $G_{K\to 0} = \langle 0|W_{K^0}(t_K)Q_i(t)|0\rangle$ in (40). The notations are the same as for Fig. 1. The contractions for the operators Q_i are given by

$$\text{for } (\bar{s}d)(\bar{u}u) = Q_{1,2}$$
$$G_{K\to 0} = -\mathrm{V}_2, \tag{60}$$

$$\text{for } (\bar{s}d)(\bar{u}u + \bar{d}d + \bar{s}s) = Q_{3,4,5,6}$$
$$G_{K\to 0} = -2\cdot \mathrm{V}_2 + \mathrm{V}_1 - \mathrm{V}_2^s + \mathrm{V}_1^s, \tag{61}$$

$$\text{for } (\bar{s}d)(\bar{u}u - \bar{d}d/2 - \bar{s}s/2) = Q_{7,8,9,10}$$
$$G_{K\to 0} = (-\mathrm{V}_2 - \mathrm{V}_1 + \mathrm{V}_2^s - \mathrm{V}_1^s)/2, \tag{62}$$

where $\Gamma_{1,2}$ and T_{abcd} in each contractions should be chosen according to (42)–(45) for each operator. We can obtain the mixing coefficient of the lower dimensional operator α_i in (39) by dividing these by the time correlation function $\langle 0|W_{K^0}(t_K)P(t)|0\rangle$ as (40).

The $K \to \pi\pi$ time correlation function for the operator $P = \bar{s}\gamma_5 d$ is calculated by

$$G_P^I(t) = \frac{1}{T}\sum_{\delta=0}^{T-1}\langle 0|W_{K^0}(t_K+\delta)P(t+\delta) \times W_{\pi\pi}^I(t_\pi+\delta, t_\pi+1+\delta)|0\rangle = -\frac{3}{\sqrt{6}}\mathrm{T}_P, \tag{63}$$

where $\mathrm{T}_P = \mathrm{III}_P - \mathrm{IV}_P$, and the contractions III_P and IV_P are shown in Fig. 3. For the contractions IV_P, the contribution of the vacuum diagram $\langle 0|K(t_K)P(t)|0\rangle \times \langle 0|W_{\pi\pi}^I(t_\pi, t_\pi+1)|0\rangle$ is supposed to be subtracted.

The $K \to \pi\pi$ time correlation for the subtracted operator $\bar{Q}_i = Q_i - \alpha_i \cdot P$ is given by subtracting the contributions of $\alpha_i \cdot P$ from those of the operator Q_i. We write these subtractions as

$$\mathrm{III} \to \mathrm{III} - \alpha_\mathrm{i}\frac{-3}{\sqrt{6}}\mathrm{III_P}, \tag{64}$$

$$\mathrm{IV} \to \mathrm{IV} - \alpha_\mathrm{i}\frac{-3}{\sqrt{6}}\mathrm{IV_P}, \tag{65}$$

dividing into the connected (III and III_P) and the disconnected contractions (IV and IV_P), where III means the total contribution from the two contractions III_i and III_i^s for $i = 1, 2$, and, similarly, for IV.

D. Calculation of quark loop

The quark loop at the weak operator $Q(x, x)$, i.e., the quark propagator starting from the position of the weak operator and ending at the same position, appears in the quark contractions III, IV, III^s, and IV^s for the $K \to \pi\pi$ process, and V and V^s for the $K \to 0$ process, as shown in the previous subsection. We calculate them by the stochastic method with the hopping parameter expansion technique (HPE) and the truncated solver method (TSM) proposed in Ref. [13].

The Wilson fermion action can be written as

$$S^W = \bar{\psi}W\psi = \bar{\psi}(M - D)\psi = \bar{\psi}M(1 - \bar{D})\psi, \tag{66}$$

where $\bar{D} = M^{-1}D$ and

$$(M\psi)(x) = (1 - \kappa C_{SW}(\sigma\cdot F(x))/2)\psi(x), \tag{67}$$

$$(D\psi)(x) = \left(\sum_\mu (D_\mu^+ + D_\mu^-)\psi\right)(x), \tag{68}$$

$$(D_\mu^+\psi)(x) = \kappa(1-\gamma_\mu)U_\mu(x)\psi(x+\mu), \tag{69}$$

$$(D_\mu^-\psi)(x) = \kappa(1+\gamma_\mu)U_\mu^\dagger(x-\mu)\psi(x-\mu). \tag{70}$$

The quark field of the Wilson fermion ψ is related to that in the continuum theory ψ^c by $\psi^c = \sqrt{2\kappa}\cdot\psi$ in the tree order.

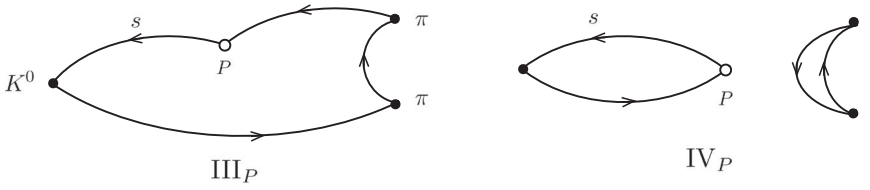

FIG. 3. Quark contractions for the time correlation function for the $K \to \pi\pi$ process for the operator $P = \bar{s}\gamma_5 d$.

From (66), the quark propagator Q can be written by a hopping parameter expansion form as

$$Q = W^{-1} = \sum_{n=0}^{\infty} \bar{D}^n M^{-1} = \sum_{n=0}^{k-1} \bar{D}^n M^{-1} + \bar{D}^k W^{-1}, \quad (71)$$

for any integer value of k. We use this expansion to calculate the quark loop $Q(x,x)$ at the weak operator. In this case, the terms with odd power of $\bar{D}$ do not contribute, thus

$$Q(x,x) = (M^{-1} + \bar{D}^2 M^{-1} + \bar{D}^4 W^{-1})(x,x), \quad (72)$$

for $k = 4$. We can replace $\bar{D}^2$ term by

$$\bar{D}_{2L} = \sum_{\mu} (\bar{D}^+_\mu \bar{D}^-_\mu + \bar{D}^-_\mu \bar{D}^+_\mu), \quad (73)$$

with $\bar{D}^\pm_\mu = M^{-1} D^\pm_\mu$. Using these expressions, we calculate the quark loop by the stochastic method according to

$$Q(\mathbf{x},t;\mathbf{x},t) = \frac{1}{N_R} \sum_{i=1}^{N_R} \xi_i^*(\mathbf{x},t) S_i(\mathbf{x},t). \quad (74)$$

The function $S_i(\mathbf{x},t)$ is defined by

$$S_i(\mathbf{x},t) = \sum_{\mathbf{y}} (M^{-1} + \bar{D}_{2L} M^{-1} + \bar{D}^4 W^{-1})(\mathbf{x},t;\mathbf{y},t) \xi_i(\mathbf{y},t), \quad (75)$$

where we introduce an $U(1)$ noise $\xi_i(\mathbf{x},t)$ which satisfies

$$\delta^3(\mathbf{x}-\mathbf{y}) = \frac{1}{N_R} \sum_{i=1}^{N_R} \xi_i^*(\mathbf{x},t) \xi_i(\mathbf{y},t), \quad (76)$$

for $N_R \to \infty$. The effect of HPE for the quark loop is to remove the $\bar{D}$ and $\bar{D}^3$ terms in (75) explicitly which make only statistical noise. We find that HPE reduces the statistical error of the decay amplitudes to about 50% compared with the normal stochastic method.

We also implement the truncated solver method (TSM) for (74) by

$$Q(\mathbf{x},t;\mathbf{x},t) = \frac{1}{N_R} \sum_{i=1}^{N_R} \xi_i^*(\mathbf{x},t)[S_i(\mathbf{x},t) - S_i^T(\mathbf{x},t)] + \frac{1}{N_T} \sum_{i=N_R+1}^{N_R+N_T} \xi_i^*(\mathbf{x},t) S_i^T(\mathbf{x},t), \quad (77)$$

where $S_i^T(\mathbf{x},t)$ is a value given with the quark propagator W^{-1} in (75) calculated with a loose stopping condition, and $S_i(\mathbf{x},t)$ is that with a stringent condition. We set $N_T = 5$ and the stopping condition $R \equiv |Wx - \xi|/|\xi| < 1.2 \times 10^{-6}$ with x denoting the iterative solution of $Wx = \xi$ for $S_i^T(\mathbf{x},t)$, and $N_R = 1$ and $R < 10^{-14}$ for $S_i(\mathbf{x},t)$ in the present work. The numerical cost of TSM (77) is about twice of that without TSM (74) with $N_R = 1$.

E. Time correlation function for $\pi\pi \to \pi\pi$

We calculate two types of time correlation functions for $\pi\pi \to \pi\pi$ to obtain the normalization factors which are needed to extract the matrix elements $\langle K|\bar{Q}_i|\pi\pi;I\rangle$ from the time correlation function $G_i^I(t)$ in (29). These are point-wall and wall-wall time correlation functions, which are defined by

$$G^I_{PW}(t) = \frac{1}{T} \sum_{\delta=0}^{T-1} \langle 0|(\pi\pi)^I(t+\delta) W^I_{\pi\pi}(t_\pi + \delta, t_\pi + 1 + \delta)|0\rangle, \quad (78)$$

$$G^I_{WW}(t) = \frac{1}{T} \sum_{\delta=0}^{T-1} \langle 0|W^I_{\pi\pi}(t+\delta, t+1+\delta) \times W^I_{\pi\pi}(t_\pi+\delta, t_\pi+1+\delta)|0\rangle, \quad (79)$$

where $(\pi\pi)^I(t)$ is the operator for the two-pion system with the isospin I,

$$(\pi\pi)^{I=2}(t) = \sum_{\mathbf{x},\mathbf{y}} (\pi^0(\mathbf{x},t)\pi^0(\mathbf{y},t) + \pi^+(\mathbf{x},t)\pi^-(\mathbf{y},t))/\sqrt{3}, \quad (80)$$

$$(\pi\pi)^{I=0}(t) = \sum_{\mathbf{x},\mathbf{y}} (-\pi^0(\mathbf{x},t)\pi^0(\mathbf{y},t)/\sqrt{2} + \sqrt{2}\pi^+(\mathbf{x},t)\pi^-(\mathbf{y},t))/\sqrt{3}, \quad (81)$$

with the operator for π^i meson $\pi^i(\mathbf{x},t)$ defined by

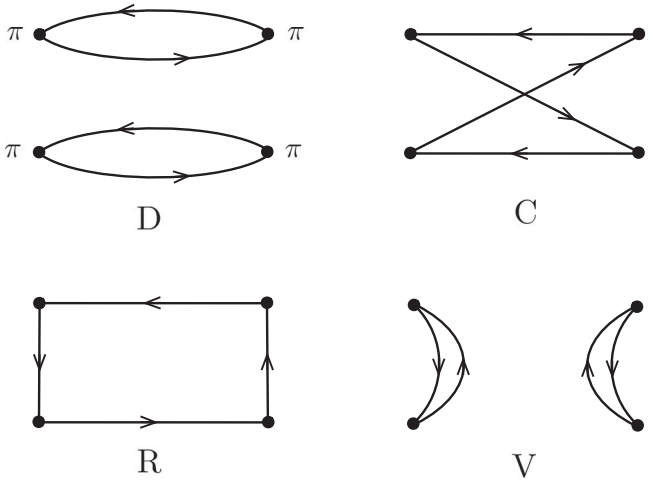

FIG. 4. Quark contractions for the time correlation function for $\pi\pi \to \pi\pi$.

$$\pi^+(\mathbf{x},t) = -\bar{d}(\mathbf{x},t)\gamma_5 u(\mathbf{x},t), \tag{82}$$

$$\pi^0(\mathbf{x},t) = (\bar{u}(\mathbf{x},t)\gamma_5 u(\mathbf{x},t) - \bar{d}(\mathbf{x},t)\gamma_5 d(\mathbf{x},t))/\sqrt{2}, \tag{83}$$

$$\pi^-(\mathbf{x},t) = \bar{u}(\mathbf{x},t)\gamma_5 d(\mathbf{x},t). \tag{84}$$

The operator $W^I_{\pi\pi}(t_1,t_2)$ $(I=0,2)$ is defined by (34) and (35). In the present work, we set $t_\pi = 0$ in (78) and (79).

In Fig. 4, we list all of the possible quark contractions for the time correlation function for the $\pi\pi \to \pi\pi$ processes. Time runs from right to left in the diagrams. There are four types of contractions, D, C, R, and V. The filled circles represent the wall source W_{π^i} in (36)–(38) or the point source π^i in (82)–(84) for the pion. For the contraction V, the contribution of the vacuum diagram, $\langle 0|(\pi\pi)^I(t)|0\rangle \times \langle 0|W^I_{\pi\pi}(t_\pi, t_\pi+1)|0\rangle$ or $\langle 0|W^I_{\pi\pi}(t,t+1)|0\rangle\langle 0|W^I_{\pi\pi}(t_\pi,t_\pi+1)|0\rangle$, is supposed to be subtracted.

For example, the explicit form for the contraction C for the point-wall time correlation function $G^I_{\mathrm{PW}}(t)$ in (78) is given by

$$\mathrm{C} = \left[\sum_{\mathbf{x},\mathbf{y}} \mathrm{Tr}(W_d(t_1;\mathbf{y},t)\gamma_5 W_d(\mathbf{y},t;t_2)\gamma_5 W_d(t_2;\mathbf{x},t)\gamma_5 W_d(\mathbf{x},t;t_1)\gamma_5) + (t_1 \leftrightarrow t_2)\right] \Big/ 2, \tag{85}$$

with $t_1 = t_\pi$ and $t_2 = t_\pi + 1$, and that for the wall-wall correlation function $G^I_{WW}(t)$ in (79) by

$$\mathrm{C} = [\mathrm{Tr}(W_d(t_1;t_4)\gamma_5 W_d(t_4;t_2)\gamma_5 W_d(t_2;t_3)\gamma_5 W_d(t_3;t_1)\gamma_5) + (t_1 \leftrightarrow t_2) + (t_3 \leftrightarrow t_4) + (t_1 \leftrightarrow t_2, t_3 \leftrightarrow t_4)]/4, \tag{86}$$

with $t_1 = t_\pi$, $t_2 = t_\pi + 1$, $t_3 = t$, $t_4 = t+1$, where the trace is taken for the color and the spin indices. The wall source propagators W_d are defined by (47)–(49).

For the calculation of the contraction R for the point-wall time correlation function $G^I_{PW}(t)$ in (78), we use the stochastic method according to

$$\mathrm{R} = \left[\frac{1}{N_R}\sum_{i=1}^{N_R}\sum_{\mathbf{x},\mathbf{y}} \mathrm{Tr}(W_d(t_1;t_2)\gamma_5 W_d(t_2;\mathbf{x},t)\gamma_5 Z_i(\mathbf{x},t)\xi_i^*(\mathbf{y},t)\gamma_5 W_d(\mathbf{y},t;t_1)\gamma_5) + (t_1 \leftrightarrow t_2)\right] \Big/ 2, \tag{87}$$

with $t_1 = t_\pi$ and $t_2 = t_\pi + 1$, where $\xi_i(\mathbf{y},t)$ is an $U(1)$ noise which satisfies (76), and $Z_i(\mathbf{x},t)$ is defined by

$$Z_i(\mathbf{x},t) = \sum_{\mathbf{y}} W^{-1}(\mathbf{x},t;\mathbf{y},t)\xi_i(\mathbf{y},t), \tag{88}$$

with the kernel of the Wilson fermion W in (66). The contraction V is also calculated by using $Z_i(\mathbf{x},t)$. In actual calculations, we find that relaxing the stopping condition to $|Wx-\xi|/|\xi| < 1.2\times 10^{-6}$ for the calculation of $Z_i(\mathbf{x},t)$ makes only negligible effects to the final result, compared with the statistical error. Thus, we adopt this loose stopping condition with $N_R = 6$ in (87).

The quark contraction for the time correlation function, $G^I_{PW}(t)$ or $G^I_{WW}(t)$, is given by

$$G^{I=2} = \mathrm{D} - \mathrm{C}, \tag{89}$$

$$G^{I=0} = \mathrm{D} + \frac{1}{2}\mathrm{C} - 3\,\mathrm{R} + \frac{3}{2}\mathrm{V}. \tag{90}$$

IV. RESULTS

A. Time correlation function for $\pi\pi \to \pi\pi$

Figure 5 shows the contributions of the four types of contractions, D, C, R, V, for the time correlation function for $\pi\pi \to \pi\pi$, with those for the point-wall function $G^I_{PW}(t)$ in (78) plotted on the left and those for the wall-wall function $G^I_{WW}(t)$ in (79) on the right panel. The source operator is placed at $t_\pi = 0$. The time correlation functions behave in the large time region as

$$G^I_{PW}(t) = A^I \cdot (\mathrm{e}^{-E^I_{\pi\pi}t} + \mathrm{e}^{-E^I_{\pi\pi}(T-t)}) + C^I, \tag{91}$$

$$G^I_{WW}(t) = A^I_{\pi\pi} \cdot (\mathrm{e}^{-E^I_{\pi\pi}t} + \mathrm{e}^{-E^I_{\pi\pi}(T-t)}) + D^I, \tag{92}$$

where $E^I_{\pi\pi}$ is the energy of the two-pion system with the isospin I, A^I is a constant whose form is irrelevant, and

$$A^I_{\pi\pi} = \langle 0|W^I_{\pi\pi}(0,1)|\pi\pi;I\rangle^2/\langle \pi\pi;I|\pi\pi;I\rangle. \tag{93}$$

The constant terms C^I and D^I in (91) and (92) come from the two pions propagating in the opposite time directions (*i.e.,* around-the-world effect for the two-pion operator).

The effective mass of the point-wall time correlation function $G^I_{PW}(t)$ is plotted in Fig. 6, where the effective mass m_{eff} at t is given by

$$\frac{G^I_{PW}(t+1) - G^I_{PW}(t+4)}{G^I_{PW}(t) - G^I_{PW}(t+3)} = \frac{f(t+1;m_{\mathrm{eff}}) - f(t+4;m_{\mathrm{eff}})}{f(t;m_{\mathrm{eff}}) - f(t+3;m_{\mathrm{eff}})}, \tag{94}$$

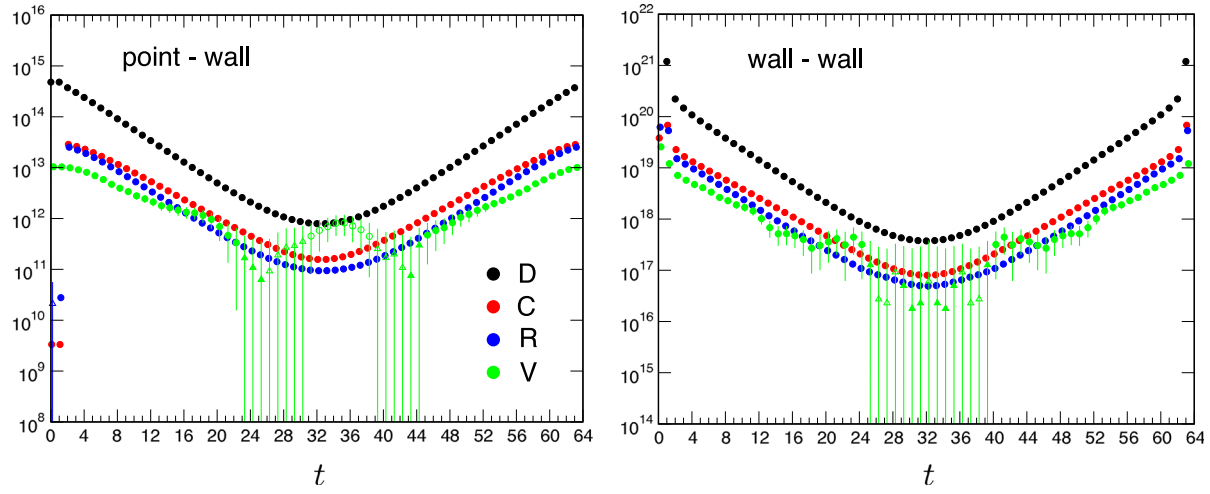

FIG. 5 (color online). Four types of contractions for the time correlation function for $\pi\pi \to \pi\pi$. Left panel shows those for the point-wall function $G^I_{PW}(t)$ in (78) and right for the wall-wall function $G^I_{WW}(t)$ in (79).

with the function $f(t; m_{\rm eff}) = \exp(-m_{\rm eff} \cdot t) + \exp(-m_{\rm eff} \cdot (T-t))$. We find plateaus in the time region $t \geq 9$ for both $I = 0$ and 2, albeit admittedly much noisier for $I = 0$ than for $I = 2$. Compared with the value $2m_\pi$ plotted in blue, the two-pion energy for $I = 2$ is larger, signifying repulsive interaction of the two-pion system, whereas that for $I = 0$ is smaller showing attractive interaction.

In the extraction of the matrix elements $\langle K|\bar{Q}_i|\pi\pi; I\rangle$ from the time correlation function $G^I_i(t)$ in (29), the values of $E^I_{\pi\pi}$ and $A^I_{\pi\pi}$ are needed. Since the statistical error of the point-wall correlation function $G^I_{PW}(t)$ is smaller than that for the wall-wall function $G^I_{WW}(t)$, we first extract the energy $E^I_{\pi\pi}$ from $G^I_{PW}(t)$ and then extract the amplitude $A^I_{\pi\pi}$ from $G^I_{WW}(t)$ by fitting to (92) with the determined value of $E^I_{\pi\pi}$ and regarding $A^I_{\pi\pi}$ and D^I as unknown parameters. The results for $E^I_{\pi\pi}$ and $A^I_{\pi\pi}$ are

$$E^{I=2}_{\pi\pi} = 0.2567(14), \qquad A^{I=2}_{\pi\pi} = 2.513(27) \times 10^{20},$$
$$E^{I=0}_{\pi\pi} = 0.2499(83), \qquad A^{I=0}_{\pi\pi} = 2.41(13) \times 10^{20}, \qquad (95)$$

in the lattice unit, where we adopt the fitting range $t = [9, 32]$ for $I = 2$ and $t = [9, 12]$ for $I = 0$.

The mass of the pion and the K meson obtained in the present work are $m_\pi = 0.12671(71)$ and $m_K = 0.26641(58)$ in the lattice unit. The energy difference between the initial K meson and the final two-pion state, $\Delta E^I = m_K - E^I_{\pi\pi}$, is $\Delta E^{I=2} = 0.0097(14)$ [21(3) MeV] and $\Delta E^{I=0} = 0.0165(83)$ [36(18) MeV]. In the present work, we assume that these violations of energy conservation yield only small effects to the results for the $K \to \pi\pi$ decay amplitudes.

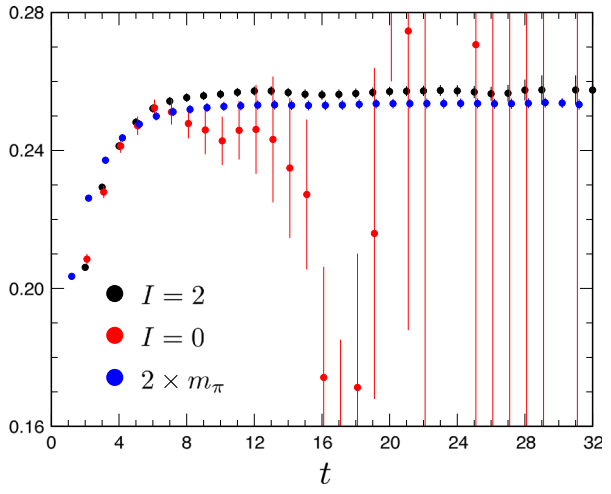

FIG. 6 (color online). Effective mass of the time correlation function $G^I_{PW}(t)$ for $\pi\pi \to \pi\pi$ with the isospin $I = 0$ and $I = 2$. Twice of the effective mass for the pion is also plotted for a comparison.

B. Time correlation function for $K \to \pi\pi$ in the $I = 0$ channel

In Fig. 7, we demonstrate the effects of the truncated solver method. The four panels 7(a)–7(d) show the contributions of the contractions III and IV to the time correlation functions for $\bar{Q}_2$ and $\bar{Q}_6$ at $t = 9$. In each panel, the data at $x = 0$ shows the result of a stochastic estimate with a stringent stopping condition, while those at $x = 1, \ldots, 6$ are obtained with a loose stopping condition, with an identical noise vector employed for $x = 0$ and $x = 1$. Thus, the difference between the data at $x = 0$ and $x = 1$ corresponds to the first term of (77) for $N_R = 1$, and the data at $x = 2, \ldots, 6$ $(N_T = 5, N_T + N_R = 6)$ correspond to the components of the second term of (77). We find that the first term is negligible compared with the statistical error for all channels. Thus, we can neglect it and estimate the quark loop contribution by only the second term as

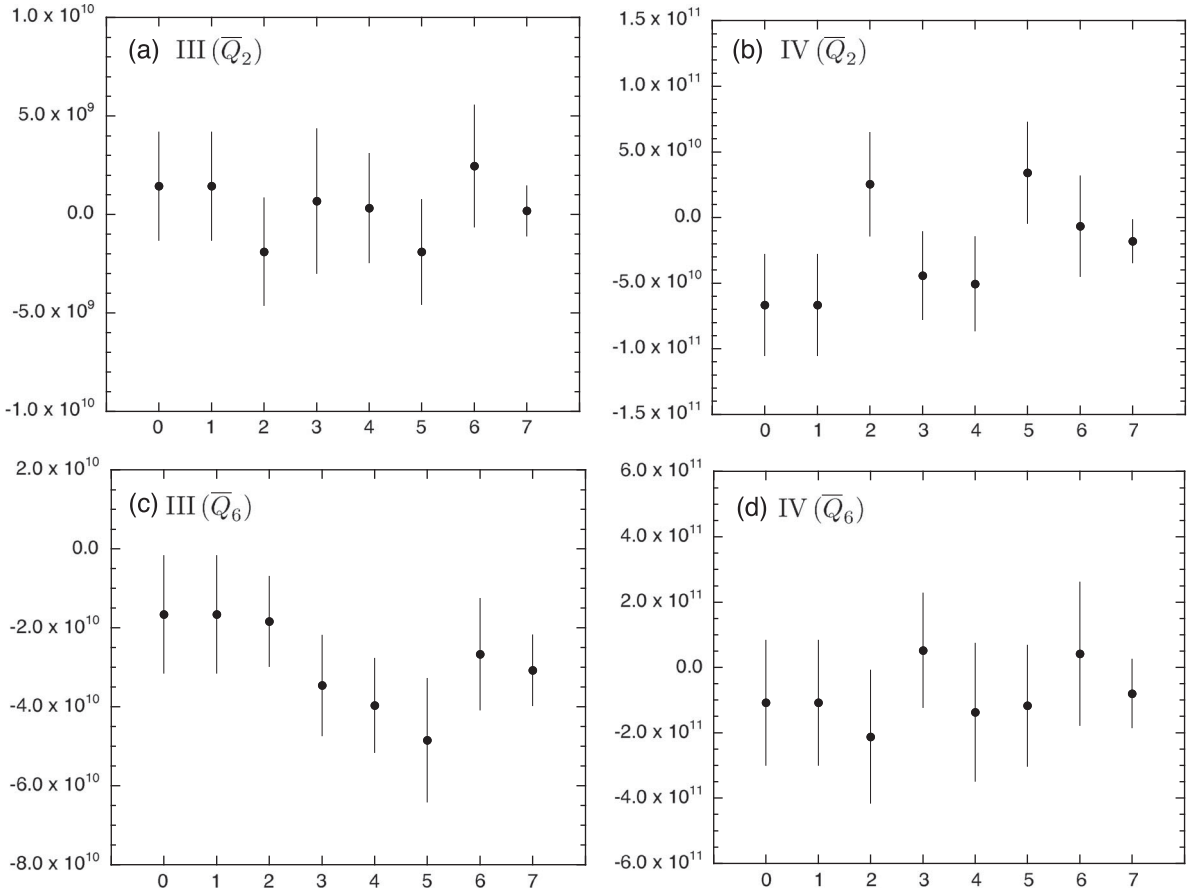

FIG. 7. Effect of the truncated solver method. Panels 7(a)–7(d) show the contributions of the contraction III and IV to the time correlation functions for $\bar{Q}_2$ and $\bar{Q}_6$ at $t = 9$. In each panel, the data at $x = 0$ show the contribution obtained by the usual stochastic method (74) with $N_R = 1$, *i.e.*, the contribution given by setting the quark loop $Q(\mathbf{x}, t; \mathbf{x}, t) = \xi_i^*(\mathbf{x}, t) S_i(\mathbf{x}, t)$ for $i = 1$. The data at $x = 1, 2, \ldots, 6$ correspond to the contributions given by setting $Q(\mathbf{x}, t; \mathbf{x}, t) = \xi_i^*(\mathbf{x}, t) S_i^T(\mathbf{x}, t)$ for $x = i = 1, 2, \ldots, 6$ $(N_R + N_T = 1 + 5)$ with $S_i^T(\mathbf{x}, t)$ in (77). The data at $x = 7$ are average of the data at $x = 1, 2, \ldots, 6$.

$$Q(\mathbf{x}, t; \mathbf{x}, t) = \frac{1}{N_T + N_R} \sum_{i=1}^{N_T+N_R} \xi_i^*(\mathbf{x}, t) S_i^T(\mathbf{x}, t). \quad (96)$$

The contribution given by the sum (96) is plotted at $x = 7$ in each panel. We see that the statistics is significantly improved by increasing the number of random numbers from 1 to 6.

The results for the $I = 0$ $K \to \pi\pi$ time correlation function for the operator Q_2 [$G_2^{I=0}(t)$ in (29)] are plotted in Fig. 8. The time slice of the two pion is set at $t_\pi = 0$ and the K meson at $t_K = 24$, while the operator $Q_i(t)$ runs over the whole time extent as explained before. In the panels 8(a) and 8(b), we observe a large cancellation between the contributions from the operator Q_2 and the subtraction term $\alpha_2 \cdot P$ for both contractions III and IV. In panel 8(c), we find that the contribution from the contraction IV is similar in magnitude to that from the contraction I. This appears different from the previous work by RBC-UKQCD Collaboration with the domain wall fermion action in Refs. [3,4]. In panel 8(d), we compare the correlation functions calculated with TSM and without TSM. We find that TSM significantly improves the statistics. The numerical cost of TSM is about twice of that without TSM. Thus, TSM is a very efficient method.

The results for Q_6 in the $I = 0$ channel are plotted in Fig. 9. Here, also, we find a large cancellation between the contributions of Q_6 and the subtraction $\alpha_6 \cdot P$ for both contractions III and IV [see panels 9(a) and 9(b)]. In panel 9(c), a large cancellation is observed between the contraction I and II, which is not the case for $\bar{Q}_2$. An efficiency of TSM is observed also for Q_6 in panel 9(d).

C. $K \to \pi\pi$ matrix elements

In order to extract the $K \to \pi\pi$ matrix element, we consider an effective matrix element $M_i^I(t)$, which behaves as $M_i^I(t) = M_i^I \equiv \langle K | \bar{Q}_i(\mathbf{0}, 0) | \pi\pi; I \rangle$ in the time region $t_K \gg t \gg t_\pi$. It can be constructed from the time correlation function $G_i^I(t)$ in (29) by

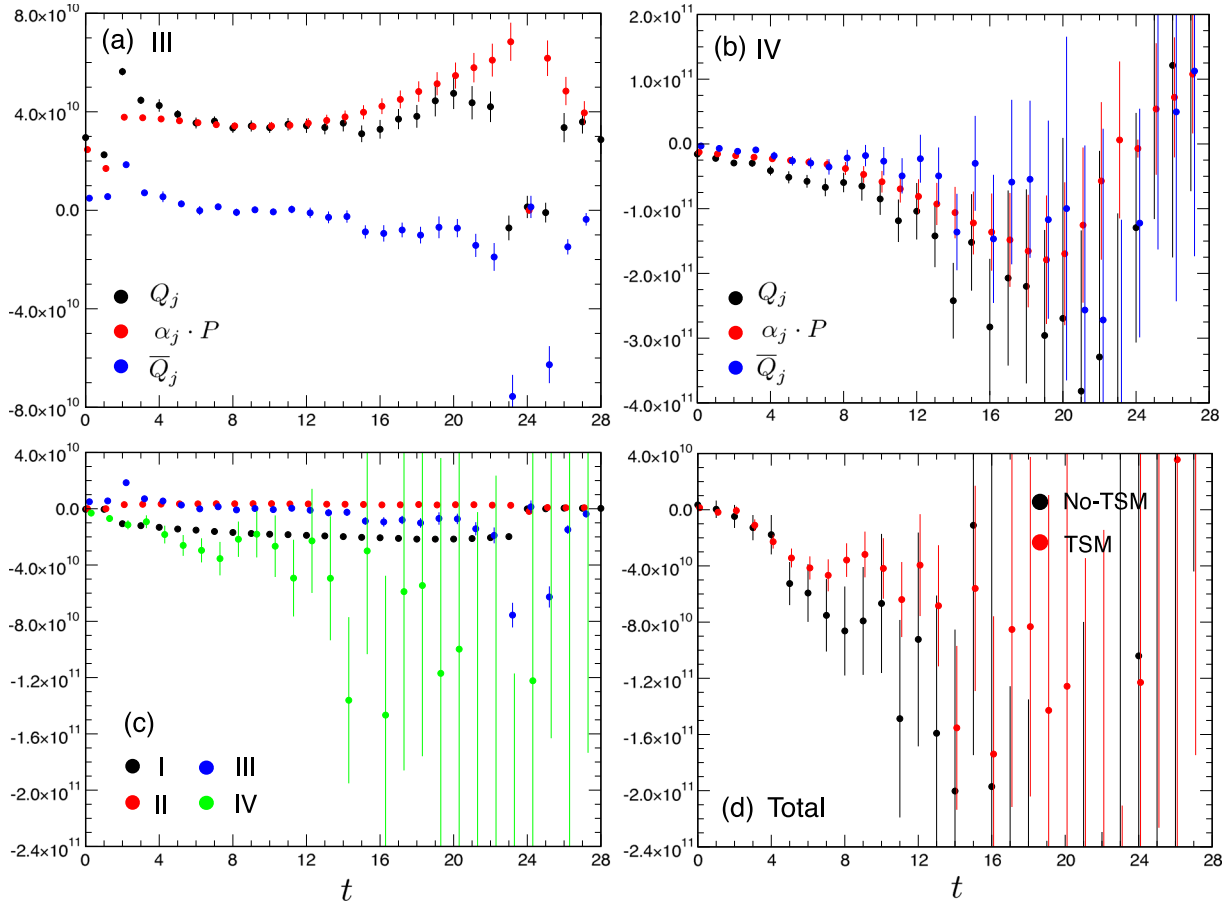

FIG. 8 (color online). Time correlation function for the operator Q_2 for the $\Delta I = 1/2$ $K \to \pi\pi$ process, $G_2^{I=0}(t)$ in (29). The time slices of the two pion and the K meson are set at $t_\pi = 0$ and $t_K = 24$, while the operator Q_i runs over the whole time extent. (a) Contributions of the contraction III for Q_2, $\alpha_2 \cdot P$ and $\bar{Q}_2 = Q_2 - \alpha_2 \cdot P$. (b) Contributions of the contraction IV for Q_2, $\alpha_2 \cdot P$ and $\bar{Q}_2 = Q_2 - \alpha_2 \cdot P$. (c) Contributions from each type of contractions for $\bar{Q}_2$. (d) Total correlation functions calculated with TSM and without TSM.

$$M_i^I(t) = G_i^I(t)/\sqrt{A_K A_{\pi\pi}^I} \cdot F^I \cdot \mathrm{e}^{m_K(t_K - t) + E_{\pi\pi}^I(t - t_\pi)} \times (-1). \tag{97}$$

Here, the K meson mass m_K and the energy of the two-pion state $E_{\pi\pi}^I$ are fixed at the values obtained from the correlation function of the K meson and the $\pi\pi \to \pi\pi$. The factor (-1) comes from the convention of the K^0 operator in (31). The constant $A_K = \langle 0|W_K|K\rangle^2/\langle K|K\rangle$ is estimated from the wall-wall propagator of the K meson, with the value $A_K = 8.949(34) \times 10^9$ in the lattice unit. The constant $A_{\pi\pi}^I$ is defined by (93) and its value is given by (95). The dimensionless constant F^I is the Lellouch-Lüscher factor [14] given by

$$\begin{aligned}(F^I)^2 &= \langle K|K\rangle \cdot \langle \pi\pi; I|\pi\pi; I\rangle/V^2 \\ &= (4\pi)\left(\frac{(E_{\pi\pi}^I)^2 m_K}{p^3}\right)\left(p\frac{\partial\delta^I(p)}{\partial p} + q\frac{\partial\phi(q)}{\partial q}\right),\end{aligned} \tag{98}$$

where V is the lattice volume $V = L^3$, $\delta^I(p)$ is the two-pion scattering phase shift for the two-pion system with the isospin I at the scattering momentum $p^2 = (E_{\pi\pi}^I)^2/4 - m_\pi^2$, and $\phi(q)$ is the function defined by

$$\tan\phi(q) = -\pi^{3/2} q/Z_{00}(1; q), \tag{99}$$

with the spherical zeta function,

$$Z_{00}(s; q) = \frac{1}{\sqrt{4\pi}} \sum_{\mathbf{n} \in \mathbb{Z}^3} (n^2 - q^2)^{-s}, \tag{100}$$

at $q = p(2\pi/L)$. In the noninteracting two-pion case, the factor takes the form $(F^I)^2 \equiv (F|_{\text{free}})^2 = (2m_K V) \cdot (2m_\pi V)^2/V^2$.

For the $I = 0$ channel, the statistics in the present work is not sufficient to obtain the scattering phase shift. We therefore use the factor for the noninteracting case, leaving a precise estimation of the factor to study in the future. For the $I = 2$ case, the phase shift is obtained with a sufficient statistics at the needed momentum. Because the scattering momentum p takes a small value, $p = 2.053(97) \times 10^{-2}$ [44.7(2.1) MeV] in our case, the phase shift can be approximated by $\delta^{I=2}(p) = p(\partial\delta^{I=2}(p)/\partial p) + \mathrm{O}(p^3)$.

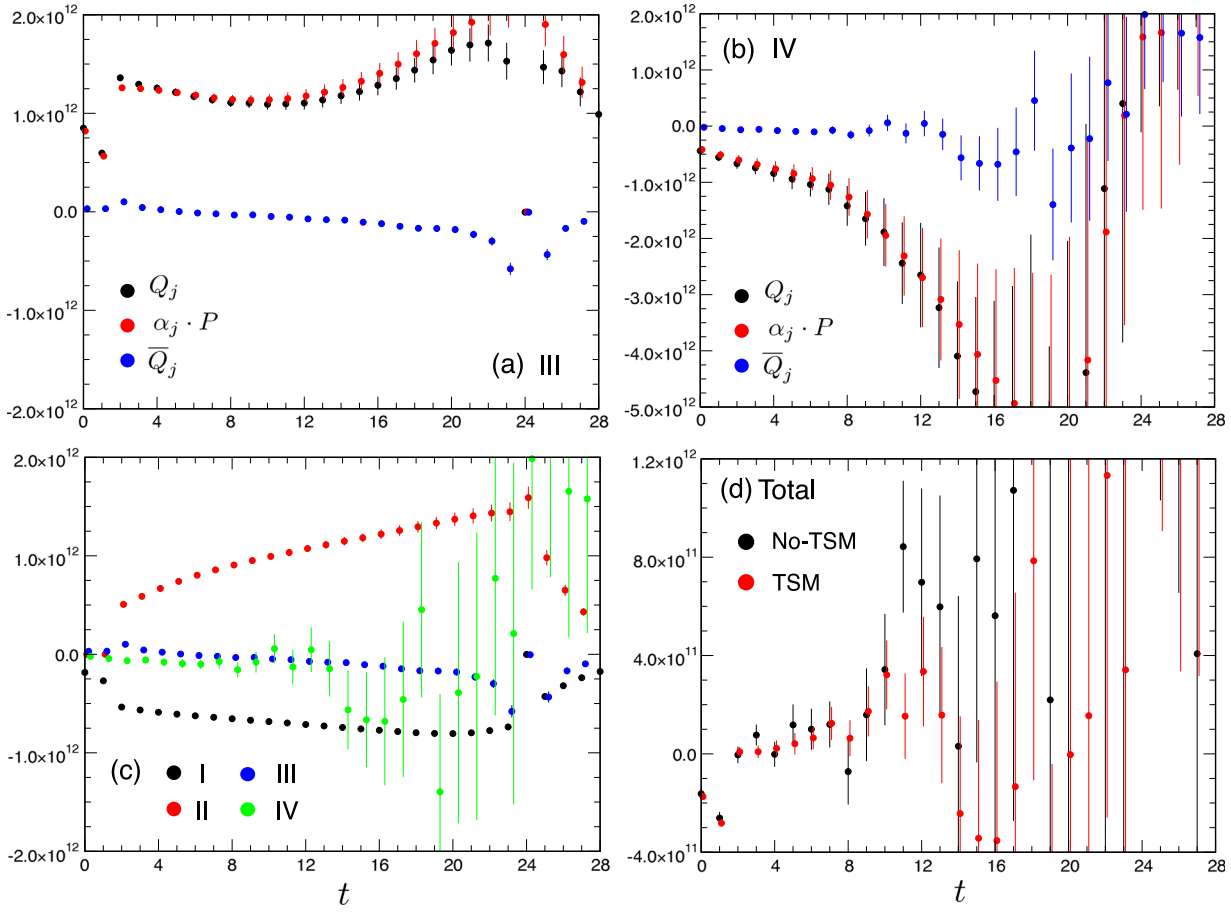

FIG. 9 (color online). Time correlation function for the operator Q_6 for the $\Delta I = 1/2$ $K \to \pi\pi$ process, $G_6^{I=0}(t)$ in (29), following the same convention as in Fig. 8.

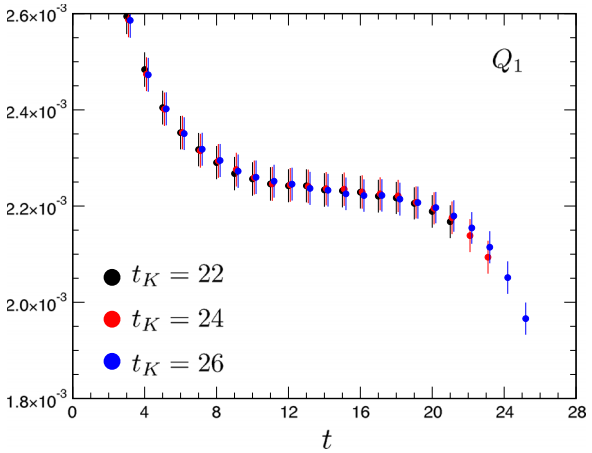

FIG. 10 (color online). Effective matrix element of $M_1^{I=2}(t)$ in (97) in the lattice unit. The time slice of the two pion is set at $t_\pi = 0$. The operator $Q_i(t)$ runs over the whole time extent. The matrix elements given with the K meson at time slice $t_K = 22, 24, 26$ are plotted.

We neglect the cubic term and find $F^{I=2}/F|_{\text{free}} = 0.9254(62)$.

Our results for the effective matrix elements for several representative channels are shown in Figs. 10 and 11 for $I = 2$, and in Fig. 12 for $I = 0$, where the matrix elements calculated with $t_K = 22$, 24, and 26 are plotted. We find plateaux for the effective matrix elements over the time interval $t = [9, 12]$ which are independent of the value of t_K. This means that the around-the-world effect of the two-pion operator is negligible in this time region.

We extract the matrix element $M_i^I \equiv \langle K|\bar{Q}_i(\mathbf{0}, 0)|\pi\pi; I\rangle$ by a constant fit of the effective amplitude for $t_K = 24$ in the time interval $t = [9, 12]$. Our results for the $I = 2$ channel (the $\Delta I = 3/2$ process) are tabulated in the second column in Table I, where the relation among the matrix elements (54) is used. The results for the $I = 0$ channel (the $\Delta I = 1/2$ process) are tabulated in the second column in Table II. Here, we do not use the operator relations (12)–(14), and treat each of ten operators as independent.

D. $K \to \pi\pi$ decay amplitudes

The renormalized matrix elements $\bar{M}_i^I(\mu)$ are obtained from the bare matrix elements on the lattice M_j^I extracted in

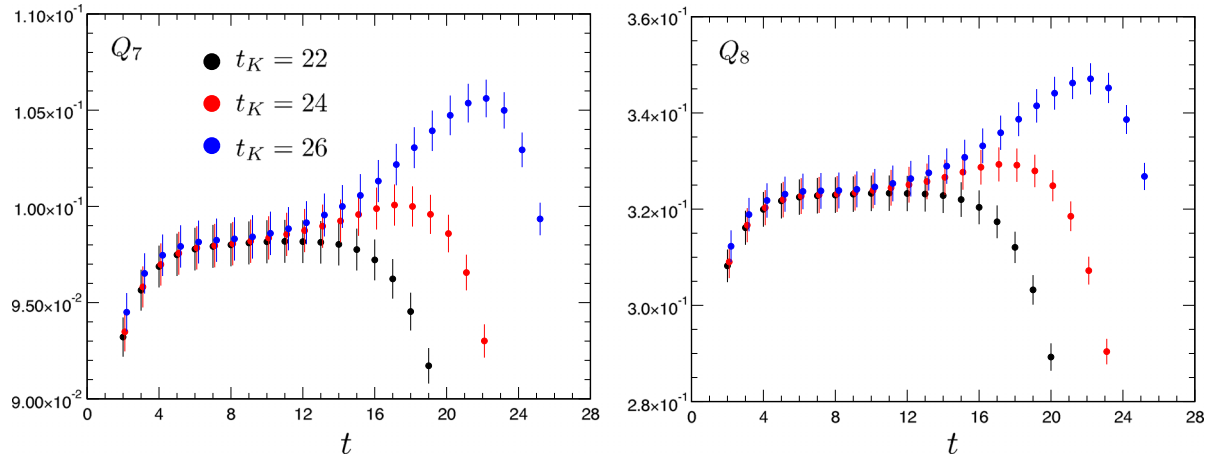

FIG. 11 (color online). Effective matrix elements of $M_{7,8}^{I=2}(t)$ in (97), following the same convention as in Fig. 10.

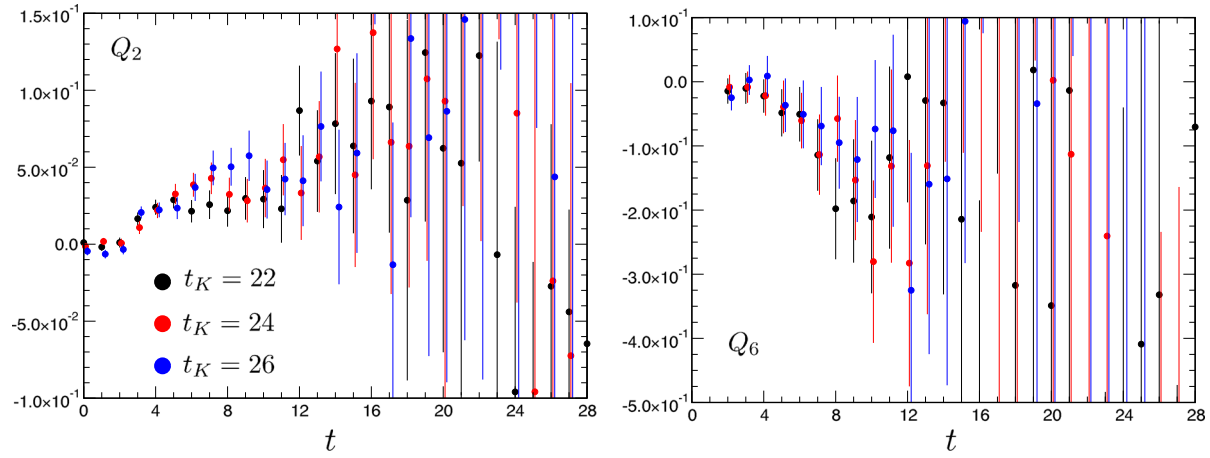

FIG. 12 (color online). Effective matrix elements of $M_{2,6}^{I=0}(t)$ in (97), following the same convention as in Fig. 10.

the previous section by multiplying with the renormalization factors as

$$\bar{M}_i^I(q^*) = \sum_{j=1}^{10} M_j^I Z_{ji}(q^* a). \tag{101}$$

The renormalization factors $Z_{ij}(q^* a)$ for our choice of the fermion and gluon actions have been calculated by perturbation theory in a one-loop order in Ref. [15]. A nonperturbatively determination is not yet available. For the renormalization in the continuum theory, we adopt the

TABLE I. Decay amplitude for the $\Delta I = 3/2$ process. The second column gives the bare matrix elements $M_i^{I=2}$ for Q_i in the lattice unit. The other columns are their contribution to A_2 [$A_2(i)$ in (105)] for $q^* = 1/a$ and π/a.

		$q^* = 1/a$		$q^* = \pi/a$	
i	M_i^I	ReA_2 (GeV)	Im$e A_2$ (GeV)	ReA_2 (GeV)	Im$e A_2$ (GeV)
1	$2.256(35) \times 10^{-3}$	$-1.887(29) \times 10^{-08}$	0	$-1.452(23) \times 10^{-08}$	0
2	$= M_1^{I=2}$	$4.330(68) \times 10^{-08}$	0	$3.920(61) \times 10^{-08}$	0
7	$9.85(11) \times 10^{-2}$	$1.053(12) \times 10^{-10}$	$2.772(32) \times 10^{-13}$	$3.172(36) \times 10^{-10}$	$2.100(24) \times 10^{-13}$
8	$3.242(37) \times 10^{-1}$	$-2.722(31) \times 10^{-10}$	$-1.670(19) \times 10^{-12}$	$-4.124(47) \times 10^{-10}$	$-1.156(13) \times 10^{-12}$
9	$= 3/2 \cdot M_1^{I=2}$	$-1.140(18) \times 10^{-12}$	$3.762(59) \times 10^{-13}$	$3.739(58) \times 10^{-12}$	$3.409(53) \times 10^{-13}$
10	$= 3/2 \cdot M_1^{I=2}$	$3.771(59) \times 10^{-10}$	$-1.756(27) \times 10^{-13}$	$4.372(68) \times 10^{-10}$	$-1.409(22) \times 10^{-13}$
Total	$\cdots$	$2.426(38) \times 10^{-08}$	$-1.192(14) \times 10^{-12}$	$2.460(38) \times 10^{-08}$	$-7.457(83) \times 10^{-13}$

TABLE II. Decay amplitude for the $\Delta I = 1/2$ process. The second column gives the bare matrix elements $M_i^{I=0}$ for Q_i in the lattice unit. The other columns are their contribution to A_0 [$A_0(i)$ in (105)] for $q^* = 1/a$ and π/a.

		$q^* = 1/a$		$q^* = \pi/a$	
i	M_i^I	ReA_0 (GeV)	ImeA_0 (GeV)	ReA_0 (GeV)	ImeA_0 (GeV)
1	$0.5(1.3) \times 10^{-2}$	$-0.4(1.1) \times 10^{-07}$	0	$-3.1(8.5) \times 10^{-08}$	0
2	$3.6(1.4) \times 10^{-2}$	$6.8(2.8) \times 10^{-07}$	0	$6.2(2.5) \times 10^{-07}$	0
3	$7.2(3.7) \times 10^{-2}$	$-1.25(65) \times 10^{-08}$	$-2.5(1.3) \times 10^{-11}$	$-1.7(8.7) \times 10^{-08}$	$-2.1(1.1) \times 10^{-11}$
4	$1.06(40) \times 10^{-1}$	$5.3(2.0) \times 10^{-08}$	$6.6(2.5) \times 10^{-11}$	$6.2(2.4) \times 10^{-08}$	$6.1(2.3) \times 10^{-11}$
5	$-1.0(4.3) \times 10^{-2}$	$1.5(5.9) \times 10^{-09}$	$1.7(6.8) \times 10^{-12}$	$1.9(7.4) \times 10^{-09}$	$1.8(7.1) \times 10^{-12}$
6	$-2.0(1.1) \times 10^{-1}$	$-8.4(4.6) \times 10^{-08}$	$-1.03(56) \times 10^{-10}$	$-7.7(4.2) \times 10^{-08}$	$-8.8(4.8) \times 10^{-11}$
7	$2.42(18) \times 10^{-1}$	$2.58(19) \times 10^{-10}$	$6.81(50) \times 10^{-13}$	$7.79(57) \times 10^{-10}$	$5.16(38) \times 10^{-13}$
8	$7.46(54) \times 10^{-1}$	$-6.26(45) \times 10^{-10}$	$-3.84(28) \times 10^{-12}$	$-9.48(68) \times 10^{-10}$	$-2.66(19) \times 10^{-12}$
9	$-3.0(1.4) \times 10^{-2}$	$1.02(48) \times 10^{-11}$	$-3.4(1.6) \times 10^{-12}$	$-3.4(1.6) \times 10^{-11}$	$-3.1(1.4) \times 10^{-12}$
10	$0.0(1.2) \times 10^{-2}$	$0.0(1.4) \times 10^{-11}$	$-0.1(6.4) \times 10^{-13}$	$0.0(1.6) \times 10^{-11}$	$-0.1(5.2) \times 10^{-13}$
Total	⋯	$6.0(3.6) \times 10^{-07}$	$-6.7(5.6) \times 10^{-11}$	$5.6(3.2) \times 10^{-07}$	$-5.2(4.8) \times 10^{-11}$

TABLE III. Standard Model parameters used to evaluate the decay amplitudes in the present work (from Ref. [17]). $\tau = -(V_{ts}^* V_{td})/(V_{us}^* V_{ud})$ and $\Lambda_{\overline{\rm MS}}^{(5)}$ is the lambda QCD for $N_f = 5$ theory. The standard representation of the CKM matrix of Ref. [17] is adopted, where the CP violation enters entirely through a complex phase of V_{td}, thus τ.

m_Z	91.188 GeV
m_W	80.385 GeV
m_t	173 GeV
m_b	4.2 GeV
m_c	1.3 GeV
$\Lambda_{\overline{\rm MS}}^{(5)}$	0.23135 GeV
α (at $\mu = m_W$)	1/129
$\sin^2\theta_W$	0.230
G_F	1.166×10^{-5} GeV^{-2}
V_{ud}	0.97427
V_{us}	0.22534
Re(τ)	0.001513
Im(τ)	−0.000601

modified minimal subtraction scheme ($\overline{\rm MS}$) with naive dimensional regularization scheme (NDR). We choose two values $q^* = 1/a$ and π/a as the matching scale from the lattice to the continuum theory in order to estimate the systematic error coming from the higher orders of perturbation theory. Large tadpole contributions in the renormalization factors for the lattice perturbation theory are subtracted by the mean-field improvement. We use a mean-field improved value in the $\overline{\rm MS}$ scheme for the coupling constant, which is given from the bare coupling constant g^2 by

$$1/g^2_{\overline{\rm MS}}(q^*) = (C_0 P + 8C_1 R)/g^2 - 0.1006 + 0.03149 \cdot N_f + (11 - 2N_f/3)/(8\pi^2) \cdot \log(q^* a) \qquad (102)$$

for our gluon and fermion actions, where $C_0 = 1 - 8C_1$ and $C_1 = -0.331$ are the parameters in the gluon action, and P is the expectation value of the plaquette, and R is that of the 1×2 Wilson loop. The detail of the procedure was discussed in Ref. [16]. From the values $P = 0.572059(31)$ and $R = 0.338902(47)$ given in Ref. [10], we obtain $g^2_{\overline{\rm MS}} = 2.699$ at $q^* = 1/a$ and $g^2_{\overline{\rm MS}} = 1.996$ at $q^* = \pi/a$.

The decay amplitudes A_I ($I = 0, 2$) are calculated from (1) as

$$A_I = \sum_{i,j=1}^{10} \bar{M}_i^I(q^*) U_{ij}(q^*, \mu) C_j(\mu), \qquad (103)$$

where

$$C_i(\mu) = \frac{G_F}{\sqrt{2}} (V_{us}^* V_{ud})(z_i(\mu) + \tau y_i(\mu)). \qquad (104)$$

The explicit form of the functions $z_i(\mu)$ and $y_i(\mu)$ in the NDR scheme have been given in Ref. [12]. The functions $U_{ij}(q^*, \mu)$ are the running factor of the operators Q_i from the scale q^* to μ for the number of active quark flavors equal to $N_f = 3$, which have also been given in Ref. [12]. In the present work, we set $\mu = m_c = 1.3$ GeV in (103) and evaluate the two functions $z_i(\mu)$ and $y_i(\mu)$ with the Standard Model parameters tabulated in Table III. We adopt the standard representation of the CKM matrix, in which CP violation enters entirely through the complex phase of V_{td}, thus $\tau = -(V_{ts}^* V_{td})/(V_{us}^* V_{ud})$. The values of the two functions are tabulated in Table IV.

From (101) and (103), the decay amplitudes can be written in terms of the bare matrix element M_i^I as

$$A_I = \sum_{i=1}^{10} M_i^I \bar{C}_i = \sum_{i=1}^{10} A_I(i), \quad (A_I(i) = M_i^I \bar{C}_i), \qquad (105)$$

TABLE IV. $z_i(\mu)$, $y_i(\mu)$, $\bar{z}_i$ and $\bar{y}_i$. The parameters of the Standard Model tabulated in Table III are used in the calculations. We set $\mu = m_c = 1.3$ GeV and choose two values $q^* = 1/a$ and π/a as the matching scale from the lattice to the continuum.

			$q^* = 1/a$		$q^* = \pi/a$	
i	$z_i(\mu)$	$y_i(\mu)$	$\bar{z}_i$	$\bar{y}_i$	$\bar{z}_i$	$\bar{y}_i$
1	-4.184×10^{-1}	0	-4.487×10^{-1}	0	-3.453×10^{-1}	0
2	$1.218 \times 10^{+0}$	0	$1.029 \times 10^{+0}$	0	9.321×10^{-1}	0
3	4.575×10^{-3}	2.910×10^{-2}	-9.327×10^{-3}	3.145×10^{-2}	-1.246×10^{-2}	2.629×10^{-2}
4	-1.373×10^{-2}	-5.782×10^{-2}	2.703×10^{-2}	-5.628×10^{-2}	3.173×10^{-2}	-5.108×10^{-2}
5	4.575×10^{-3}	4.869×10^{-3}	-7.309×10^{-3}	1.402×10^{-2}	-9.284×10^{-3}	1.470×10^{-2}
6	-1.373×10^{-2}	-9.009×10^{-2}	2.323×10^{-2}	-4.700×10^{-2}	2.130×10^{-2}	-4.015×10^{-2}
7	6.305×10^{-5}	-2.010×10^{-4}	5.777×10^{-5}	-2.514×10^{-4}	1.731×10^{-4}	-1.904×10^{-4}
8	0	1.098×10^{-3}	-4.573×10^{-5}	4.600×10^{-4}	-6.871×10^{-5}	3.183×10^{-4}
9	6.305×10^{-5}	-1.168×10^{-2}	-3.047×10^{-6}	-9.925×10^{-3}	7.287×10^{-5}	-8.995×10^{-3}
10	0	4.357×10^{-3}	5.277×10^{-5}	4.635×10^{-3}	6.368×10^{-5}	3.717×10^{-3}

where

$$\bar{C}_i = \sum_{j,k=1}^{10} Z_{ij}(q^* a) U_{jk}(q^*, \mu) C_k(\mu). \tag{106}$$

The constant $\bar{C}_i$ should be independent of μ and q^*, and depend only on the lattice cutoff $1/a$, if we work in the full order of perturbation theory. We define $\bar{z}_i$ and $\bar{y}_i$ by (104) for $\bar{C}_i$. The values of these quantities for $q^* = 1/a$ and π/a at $\mu = m_c = 1.3$ GeV are given in Table IV.

Our final results of the decay amplitudes are given in Table V. The direct CP violation parameter ϵ'/ϵ is obtained by

$$\mathrm{Re}(\epsilon'/\epsilon) = \frac{\omega}{\sqrt{2}|\epsilon|}\left(\frac{\mathrm{Im}A_2}{\mathrm{Re}A_2} - \frac{\mathrm{Im}A_0}{\mathrm{Re}A_0}\right), \tag{107}$$

with $\omega = \mathrm{Re}A_2/\mathrm{Re}A_0$, where the experimental value of the indirect CP violation parameter $|\epsilon| = 2.228 \times 10^{-3}$ is used in the estimation. The statistical errors are estimated by the jackknife procedure with a bin size of ten configurations (250 MD time units). We also list results of the RBC-UKQCD Collaboration at the similar quark masses ($m_\pi =$ 422 MeV [3] and 330 MeV [4]) for comparison. These two cases are calculated with the unphysical kinematics at $m_K \sim 2m_\pi$, as in our calculation. In the table, the results of the RBC-UKQCD Collaboration for the $\Delta I = 3/2$ process obtained at the physical quark mass with the physical kinematics, where the pions in the final state have finite momenta, in the continuum limit presented in Ref. [2], and the experimental values are also tabulated. We note that our results with an unphysical kinematics can not be directly compared with these values at the physical quark mass.

From Table V, we learn that the dependence on q^* is negligible for most of the decay amplitudes, but it is very large for $\mathrm{Im}A_2$. A nonperturbative determination of the renormalization factor is necessary to obtain a reliable result for this value. We find a large enhancement of the $\Delta I = 1/2$ process over that for the $\Delta I = 3/2$ at our quark mass $m_\pi = 280$ MeV. The RBC-UKQCD Collaboration found that the enhancement was explained by the following numerical mechanism [18]: A large cancellation between two dominant quark diagrams occurs for the $\Delta I = 3/2$ process, rendering $\mathrm{Re}A_2$ small, while such a cancellation does take place for the $\Delta I = 1/2$ process. We confirm this numerical mechanism also in our case.

Our result for A_0, particularly for the imaginary part, still has a large statistical error so that we do not obtain a nonzero result for $\mathrm{Re}(\epsilon'/\epsilon)$ over the error. We observe that the results for A_0 by the RBC-UKQCD Collaboration at a similar pion mass $m_\pi = 330$ MeV [4] have smaller errors

TABLE V. Results of the $K \to \pi\pi$ decay amplitudes. The results by the RBC-UKQCD Collaboration at $m_\pi = 422$ MeV [3], 330 MeV [4], the physical quark mass in the continuum limit (only for the $\Delta I = 3/2$ process) [2], and the experimental values are also tabulated.

	$q^* = 1/a$	$q^* = \pi/a$	RBC-UKQCD			Exp.
a (fm)	0.091		0.114	0.114	…	…
m_π (MeV)	280		330	422	140	140
$\mathrm{Re}A_2(\times 10^{-8}$ GeV)	2.426(38)	2.460(38)	2.668(14)	4.911(31)	1.50(4)(14)	1.479(4)
$\mathrm{Re}A_0(\times 10^{-8}$ GeV)	60(36)	56(32)	31.1(4.5)	38.0(8.2)		33.2(2)
$\mathrm{Re}A_0/\mathrm{Re}A_2$	25(15)	23(13)	12.0(1.7)	7.7(1.7)		22.45(6)
$\mathrm{Im}A_2(\times 10^{-12}$ GeV)	−1.192(14)	−0.7457(83)	−0.6509(34)	−0.5502(40)	−0.699(20)(84)	
$\mathrm{Im}A_0(\times 10^{-12}$ GeV)	−67(56)	−52(48)	−33(15)	−25(22)		
$\mathrm{Re}(\epsilon'/\epsilon)(\times 10^{-3})$	0.8(2.5)	0.9(2.5)	2.0(1.7)	2.7(2.6)		1.66(23)

than ours. This is because they use a different two-pion operator for which the wall sources for the two pions are separated by $\delta = 4$ in the time direction, and they set the fitting range closer to the two-pion source than our case in extracting the matrix elements from the time correlation functions. Improving statistics by devising a more efficient operator for the two-pion state is an important work reserved for the future.

The contributions of the bare matrix element M_i^I to the decay amplitude A_I [$A_I(i)$ in (105)] are tabulated in Table I for the $\Delta I = 3/2$ and in Table II for the $\Delta I = 1/2$ process. We find that the main contribution to $\mathrm{Re}A_2$ comes from the operator Q_1 and Q_2, and that to $\mathrm{Im}A_2$ from Q_8. The main contribution to $\mathrm{Re}A_0$ comes from the operator Q_2 and that to $\mathrm{Im}A_0$ from Q_6.

V. CONCLUSIONS

In the present work, we have shown that mixings with four-fermion operators with wrong chirality are absent even for the Wilson fermion action for the parity odd process due to CPS symmetry. Therefore, after subtraction of an effect from the lower dimensional operator, a calculation of the decay amplitudes is possible without additional calculations for the operator with wrong chirality. This is the same situation for chirally symmetric lattice actions such as the domain wall action. A potential advantage with the Wilson fermion action over chirally symmetric lattice actions is that the computational cost is generally smaller. Hence, with the same amount of computational resources, a statistical improvement may be expected.

As the first step of a study to verify the possibility of calculations, we considered the K meson decay amplitude for both the $\Delta I = 1/2$ and $3/2$ channels with the Wilson fermion action at an unphysical quark mass $m_K \sim 2m_\pi$. We have found that the stochastic method with the hopping parameter expansion technique and the truncated solver method are very efficient for variance reduction, yielding a first result for the $I = 0$ amplitude with the Wilson fermion action.

We have been able to show a large enhancement of the $\Delta I = 1/2$ process over that for the $\Delta I = 3/2$ at our quark mass [$m_\pi = 275.7(1.5)$ MeV and $m_K = 579.7(1.3)$ MeV]. However, our result for A_0, particularly for the imaginary part, still has a large statistical error so that we have not obtained a nonzero result for $\mathrm{Re}(\epsilon'/\epsilon)$ over the error. For the $I = 0$ two-pion system, the statistics in the present work are not sufficient to obtain the scattering phase shift. We therefore used the Lellouch-Lüscher factor for the noninteracting case in the calculation of the $\Delta I = 1/2$ process. Improving statistics by devising a more efficient operator for the $I = 0$ two-pion state is an important work reserved for the future.

Our calculation is carried out away from the physical quark masses, and the decay of the K meson to two zero momentum pions at $m_K \sim 2m_\pi$ is considered. Clearly, we need to work toward smaller quark masses and a more realistic kinematics in which the two pions carry finite momenta. This will be a major challenge that we now have to face.

ACKNOWLEDGMENTS

We would like to thank members of the RBC-UKQCD Collaboration for kind comments and suggestions. This research used computational resources of the K computer provided by the RIKEN Advanced Institute for Computational Science and T2K-TSUKUBA by University of Tsukuba through the HPCI System Research Project (Project ID:hp120153). This work is supported by Grants-in-Aid of the Ministry of Education No. 23340054, Interdisciplinary Computational Science Program in CCS, University of Tsukuba, and Large Scale Simulation Program No. 12-08 (FY2012) of High Energy Accelerator Research Organization (KEK).

[1] T. Blum *et al.* (RBC and UKQCD Collaborations), Phys. Rev. Lett. **108**, 141601 (2012); Phys. Rev. D **86**, 074513 (2012).
[2] T. Blum *et al.* (RBC and UKQCD Collaborations), Phys. Rev. D **91**, 074502 (2015).
[3] T. Blum *et al.* (RBC and UKQCD Collaborations), Phys. Rev. D **84**, 114503 (2011).
[4] Q. Liu (RBC and UKQCD Collaborations), *Proc. Sci.*, Lattice 2011 (2011) 287.
[5] C. Kelly and D. Zhang (RBC and UKQCD Collaborations), *Proc. Sci.*, Lattice 2014 (2014) 365; D. Zhang and C. Kelly (RBC and UKQCD Collaborations), *Proc. Sci.*, Lattice 2014 (2014) 366.
[6] C . W. Bernard, T. Draper, G. Hockney, and A. Soni, Nucl. Phys. B, Proc. Suppl. **4**, 483 (1988).
[7] A. Donini, V. Giménez, G. Martinelli, M. Talevi, and A. Vladikas, Eur. Phys. J. C **10**, 121 (1999).
[8] C. W. Bernard, T. Draper, A. Soni, H. D. Politzer, and M. B. Wise, Phys. Rev. D **32**, 2343 (1985); C. Dawson, G. Martinelli, G. C. Rossi, C. T. Sachrajda, S. Sharpe, M. Talevi, and M. Testa, Nucl. Phys. **B514**, 313 (1998).
[9] L. Maiani, G. Martinelli, G. Rossi, and M. Testa, Nucl. Phys. **B289**, 505 (1987); M. Testa, Nucl. Phys. B, Proc. Suppl. **63**, 38 (1998).
[10] S. Aoki *et al.* (PACS-CS Collaboration), Phys. Rev. D **79**, 034503 (2009).

[11] N. Ishizuka, K.-I. Ishikawa, A. Ukawa, and T. Yoshié, *Proc. Sci.*, Lattice 2013 (2013) 474; Lattice 2014 (2014) 364.
[12] For a review, see, G. Buchalla, A. J. Buras, and M. E. Lautenbacher, Rev. Mod. Phys. **68**, 1125 (1996).
[13] G. S. Bali, S. Collins, and A. Schäfer, Comput. Phys. Commun. **181**, 1570 (2010).
[14] L. Lellouch and M. Lüscher, Commun. Math. Phys. **219**, 31 (2001).
[15] Y. Taniguchi, J. High Energy Phys. 04 (2012) 143.
[16] A. A. Khan *et al.* (*CP*-PACS Collaboration), Phys. Rev. D **65**, 054505 (2002); **67**, 059901(E) (2003).
[17] J. Beringer *et al.* (Particle Data Group), Phys. Rev. D **86**, 010001 (2012).
[18] P. A. Boyle *et al.* (RBC and UKQCD Collaborations), Phys. Rev. Lett. **110**, 152001 (2013).